Self-assembly of new porous materials

by

Tia Jacobs

Submitted in partial fulfilment of the requirements for the degree

Doctor of Philosophy

at

Stellenbosch University

Department of Chemistry and Polymer Science

Faculty of Science

Supervisor: Prof. L. J. Barbour

Co-Supervisor: Dr. M. W. Bredenkamp

Date: March 2009

DECLARATION

By submitting this thesis electronically, I declare that the entirety of the work contained therein is my own, original work, that I am the owner of the copyright thereof (unless to the extent explicitly otherwise stated) and that I have not previously in its entirety or in part submitted it for obtaining any qualification.

Date: 11 February 2009

ABSTRACT

The primary objective of the work was to prepare and investigate new porous materials using the principles of crystal engineering. Both organic and metal-organic systems were studied and the work can best be divided into two separate sections:

1. The crystal engineering of Dianin's Compound, a well-known organic host.

2. The design and synthesis of a series of related porous coordination compounds consisting of discrete, dinuclear metallocycles.

The first section discusses the synthetic modification of Dianin's compound in order to engineer a new clathrate host with an altered aperture size. Although this study ultimately failed to isolate the host material in its porous guest-free form, the work led to the discovery of a chiral host framework that aligns guest molecules in a polar fashion, and consequently displays non-linear optical properties. These findings are unprecedented in the long history of crystal engineering of Dianin's compound and its analogues. This section also describes desorption studies of the new inclusion compound, as well as the known thiol analogue of Dianin's compound. Systematic characterisation of these desorbed phases has raised interesting fundamental questions about desolvation processes in general.

The second section constitutes the major portion of the work. A series of related isostructural coordination metallocycles were synthesised and their structure-property relationships were investigated using a variety of complementary techniques. These metallocyclic compounds all crystallise as solvates in their as-synthesised forms, and different results are obtained upon desolvation of the materials. In each case, desolvation occurs as a single-crystal to single-crystal transformation and three new "seemingly nonporous" porous materials were obtained. A single-crystal diffraction study under various pressures of acetylene and carbon dioxide was conducted for one of the porous metallocycles. This enabled the systematic study of the host deformation with increasing equilibrium pressure (*i.e.* with increasing guest occupancy). The observed differences in the sorption behaviour for acetylene and carbon dioxide are discussed and rationalised. Gravimetric gas sorption isotherms

were also recorded for the three different porous materials and the diffusion of bulkier molecules through the host was also investigated structurally. Finally, a possible gas transport mechanism is postulated for this type of porous material (*i.e.* seemingly nonporous), and this is supported by thermodynamic and kinetic studies, as well as molecular mechanics and statistical mechanics simulations.

OPSOMMING

Die primêre doel van die werk was om nuwe poreuse materiale te berei en deur die toepassing van beginsels van kristalmanipulasie (E. *crystal engineering*) te ondersoek. Beide organiese- en metaal-organiese sisteme is bestudeer en die werk kan in twee kategorieë verdeel word:

1. Die kristalmanipulasie van Dianin se verbinding, 'n bekende organiese gasheer.

2. Die ontwerp en sintese van 'n reeks verwante poreuse koördinasieverbindings wat uit diskrete, binukleêre metallosiklieseverbindings bestaan.

Die eerste deel handel oor die sintetiese verandering van Dianin se verbinding om 'n nuwe klatraatgasheer met 'n veranderde spleetgrootte te vorm. Alhoewel hierdie studie nie daarin geslaag het om die gasheer in sy poreuse "gas(E. *guest*)-vrye" vorm te isoleer nie, het die werk 'n nuwe chirale gasheerraamwerk aan die lig gebring. Die chirale gasheerraamwerk rig gas(E. *guest*)molekules in eendimensionele kolomme op 'n polêre wyse en gevolglik vertoon die materiaal nie-linieêre optiese eienskappe. Hierdie resultaat is ongekend in die lang geskiedenis van kristalmanipulasie van Dianin se verbindings en sy analoë. Hierdie afdeling beskryf ook die desorpsiestudies van die nuwe gasheer, en die tiol-afgeleide van Dianin se verbinding. Die sistematiese karakterisering van hierdie fases na desorpsie het fundamentale vrae na vore gebring oor desorpsieprosesse oor die algmeen.

Die tweede afdeling maak die grootste gedeelte van die werk uit. 'n Reeks verwante isostrukturele ringvormige koördinasieverbindings is gesintetiseer en hul struktuur-eienskap verhoudings is deur 'n verskeidenheid komplementêre tegnieke ondersoek. Hierdie metallosiklieseverbindings kristalliseer almal in gesolveerde toestand vanaf sintese en verskillende resultate word verkry wanneer die verbinding desorpsie ondergaan. In alle gevalle vind gas(E. *guest*)desorpsie as enkel-kristal na enkel-kristal omsettings plaas en drie nuwe 'oënskynlik nie-poreuse' poreuse materiale is bekom. 'n Enkelkristal diffraksiestudie onder verskeie gasdrukke is met asetileen en koolstofdioksied uitgevoer vir een van die poreuse metallosiklieseverbindings. Dit

het die geleentheid geskep om die mate waartoe die gasheer as gevolg van verhoogde ewewigsdruk vervorm (en dus toename in gasheerbesetting), sistematies te bestudeer. Die waargenome verskille in sorpsie-optrede vir asetileen en koolstofdioksied word bespreek en verklaar. Gravimetriese gassorpsie isoterme is ook vir die drie poreuse materiale verkry en die diffusie van groter molekules deur die gasheer is struktureel ondersoek. Laastens word 'n moontlike gasoordragmeganisme vir hierdie tipe poreuse (*i.e.* oënskynlik nie-poreuse) materiale gepostuleer. Hierdie bespreking word deur termodinamiese en kinetiese studies aangevul, sowel as molekulêre-meganika en statisties-meganiese studies.

ACKNOWLEDGEMENTS

A number of people have contributed to the completion of this thesis.

Firstly a sincere thanks to my supervisor Prof Len Barbour. He has been an excellent mentor and always full of endless ideas and good suggestions. I also want to thank my co-supervisor Dr Martin Bredenkamp who at all times helped out with synthetic advice and deciphering strange NMR peaks. Their passion and interest for chemistry and all things related to research has been contagious.

Then I want to acknowledge friends and colleagues (past and present) in the Supramolecular Chemistry Group and some former study buddies. I was probably not always the most cheerful study, lab or office partner, but these people have made my chemistry career so far very special and enjoyable since the years of undergraduate study and honours, up until the printing of this manuscript: Jacorien Coetzee, Jandré de Villiers, Gareth Lloyd, Dr Liliana Dobrańska, Dr Elijane de Vries, Dr Clive Oliver, Bettinah Chipimpi, Storm Potts, Leigh Loots, Charl Marias, Eustina Batisai, Marlene Milani, Dr Dinabandhu Das, Dr Subhadip Neogi, Dr Jan Gertenbach, Dr Tanya le Roex, Dr Catharine Esterhuysen and Dr Delia Haynes.

To my friends (some of which probably forgot what I looked like during the preparation of this thesis), my family (who were always proud even though most of them have no idea what I do) and Simon: all of your support and encouragement is appreciated.

PUBLICATIONS

1. E. J. C. Vries, M. W. Bredenkamp, T. Jacobs and G. O. Lloyd, *Acta Crystallogr., Sect. E,* **2005**, E61, o2871-2872.
2. G. O. Lloyd, J. Alen, T. Jacobs, M. W. Bredenkamp and E. J. C. de Vries, *Acta Crystallogr., Sect. E,* **2006**, E62, o691-o693.
3. T. Jacobs, G. O. Lloyd and M. W. Bredenkamp, *Acta Crystallogr., Sect. E*, **2006**, E62, o4400-o4402.
4. L. Dobrzańska, G. O. Lloyd, T. Jacobs, I. Rootman, C. L. Oliver, M. W. Bredenkamp and L. J. Barbour, *J. Molstruct.*, **2006**, 796, 107-113.
5. T. Jacobs, M. W. Bredenkamp, *Acta Crystallogr., Sect. E* , **2007**, *63*, O4444.
6. T. Jacobs, M. W. Bredenkamp, E. J. C. de Vries, *Acta Crystallogr., Sect. E***,** **2007**, *63*, 03736.

CONFERENCES

1. T. Jacobs, G. O. Lloyd, M. W. Bredenkamp and L. J. Barbour, *Supramolecular cocrystallisation : a new paradigm for the organic solid state*, 23rd European Crystallography Meeting, **2006**, Belgium, poster presentation.
2. T. Jacobs, G. O. Lloyd, L. Dobrańska and L. J. Barbour, *Molecular assembly of isostructural discrete hexagons*, 37ICCC, **2006**, South Africa, poster presentation.
3. T. Jacobs**,** *Binding gas molecules in a 'nonporous' lattice*, Inorg007, SACI Inorganic Chemistry Conference in Langebaan, **2007**, South Africa, oral presentation.
4. T. Jacobs, G. O. Lloyd, L. Dobrańska and L. J. Barbour, *Solvent diffusion and binding in a 'nonporous' single crystal*, 24th European Crystallography Meeting, **2007**, Morocco, poster presentation.

ABBREVIATIONS

0D	Zero Dimensional
ATR	Attenuated Total Reflection
CIF	Crystallographic Information File
CSD	Cambridge Structural Database
DC	Dianin's Compound
DFT	Density Functional Theory
DSC	Differential Scanning Calorimetry
E_a	Activation Energy
EDS	Energy Dispersive Spectrum
G	Guest
H	Host
H:G	Host:Guest ratio
IUPAC	International Union of Pure and Applied Chemistry
k	Rate Constant
M	Metal
MOF	Metal-organic Framework
NLO	Non-linear Optics
NMR	Nuclear Magnetic Resonance
RNA	Ribonucleic Acid

SBU	Secondary Building Units
SCD	Single-Crystal X-ray Diffraction
SCTSCT	Single-crystal to Single-crystal Transformation
SEM	Scanning Electron Microscopy
SHG	Second Harmonic Generation
T	Temperature
TGA	Thermogravimetric Analysis
TMV	Tobacco Mosaic Virus
T_{on}	Onset Temperature
XRPD	X-ray Powder Diffraction
ZSM	Zeolite Socony Mobil
$\Delta G°$	Standard Gibbs free energy
$\Delta H°_{iso}$	Standard Isosteric Heat of Adsorption
$\Delta S°$	Standard Entropy change

ATOMIC COLOR KEY


Hydrogen


Carbon

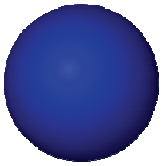
Nitrogen

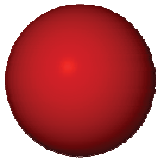
Oxygen

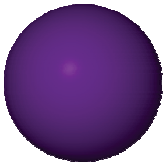
Sulphur

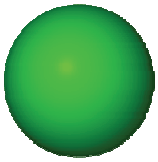
Chlorine

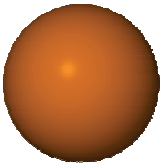
Bromine

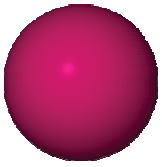
Iodine

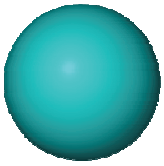
Metal

TABLE OF CONTENTS

LIST OF FIGURES

LIST OF TABLES

CHAPTER 1

GENERAL INTRODUCTION

1.1 SUPRAMOLECULAR CHEMISTRY

Molecular chemistry is described as the chemistry of atoms and the covalent bond and aims to define the rules by which the structures, properties, and transformations of molecular species are governed.[1] On the other hand, molecules can also associate with one another by means of noncovalent interactions to form entities of higher complexity. This phenomenon was first identified by K. L. Wolf when he introduced the concept of the "Übermolecule" (*i.e.* supermolecule) in the 1930s.[2-4] The term *supramolecular chemistry*[5] was first used in 1978, when Jean-Marie Lehn defined it as "…the chemistry of molecular assemblies and of the intermolecular bond."[6] The paradigm shift from molecular chemistry to supramolecular chemistry is fittingly expressed by the statement that "…supermolecules are to molecules and the intermolecular bond what molecules are to atoms and the covalent bond."[1,7] Expressed even more succinctly, the field of supramolecular chemistry is "chemistry beyond the molecule."[1] Figure 1.1 illustrates the relationship between molecular and supramolecular chemistry, where the receptor is an organic molecule (constructed by covalent synthesis) able to complex other molecular or ionic species by means of intermolecular interactions to create a supermolecule. This supermolecule is now of higher complexity and consists of two or more molecular entities.

The aim of this introduction is not to provide an all-encompassing historical perspective of the ever-expanding field of supramolecular chemistry, or even to provide a comprehensive definition. The discussion here will rather focus on the intersection of three interconnected subfields that are relevant to this study, *i.e.* crystal engineering, host:guest chemistry and porosity. It should be noted that for certain topics these partitions are subjective and, in such cases, the author's discretion has been used to present a particular topic under one subfield rather than another.

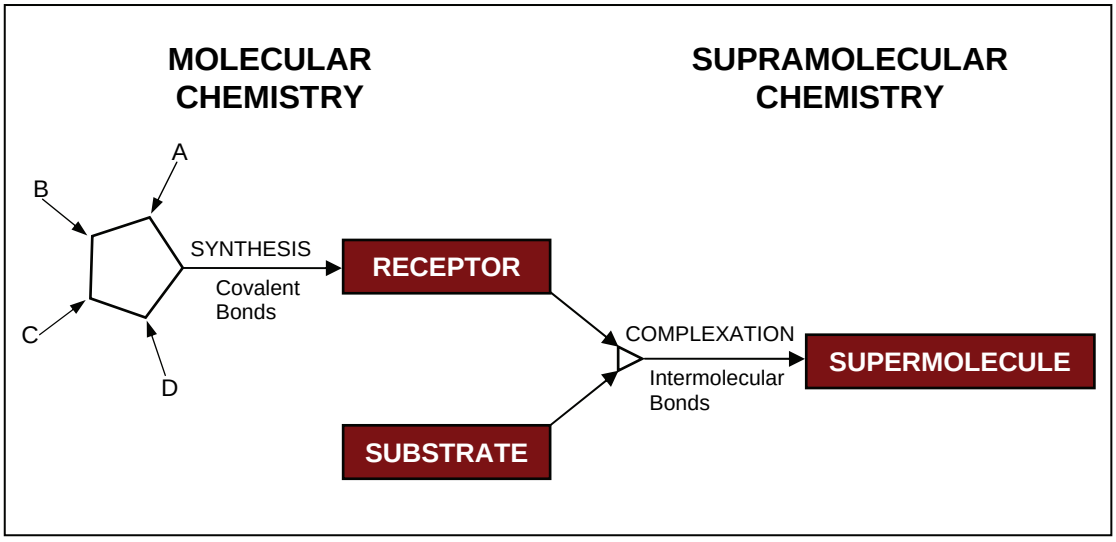

Figure 1.1 From molecular to supramolecular chemistry.[6]

For more general information on supramolecular chemistry the reader is referred to the following texts: *Comprehensive Supramolecular Chemistry*[8] (an 11-volume encyclopedia), *Supramolecular Chemistry*[9] (the first textbook on the subject), the *Encyclopedia of Supramolecular Chemistry*[10] (a two-volume encyclopedia).

"This opens wide the door to the creative imagination of the chemist at the meeting point of chemistry with biology and physics, in order not only to discover but above all to invent, to create: the score of chemistry is not just to be played but to be composed!"

J. M. Lehn[11]

1.2 CRYSTAL ENGINEERING

As a parallel to covalent synthesis, the supramolecular chemist needs to devise strategies to combine molecules into supermolecules. These strategies have to consider the energetic and geometric properties of different types of intermolecular interactions in order to effectively design and synthesise structures with desired properties.[12] Particularly with regard to the solid state, this area of chemistry has become a very active discipline within supramolecular chemistry, and is known as crystal engineering. The term was first used in 1955 when Pepinsky presented a paper entitled "Crystal Engineering: a new concept in crystallography," in which he discussed the introduction of metal-containing ions into crystals (for their anomalous dispersion properties) in order to obtain absolute structure.[13] However, it is commonly accepted that the term "crystal engineering" was introduced (and the field of crystal engineering realised) over three decades ago by Schmidt[14] in reference to photodimerisation reactions in the solid state. Schmidt went on to say in the same article about the *theory of the organic solid state:* "… Once such a theory exists we shall … be able to 'engineer' crystal structures having intermolecular contact geometry appropriate for chemical reaction …"

The concept of crystal engineering was defined by Desiraju as "…the understanding of intermolecular interactions in the context of crystal packing and in the utilisation of such understanding in the design of new solids with desired physical and chemical properties."[15] In other words, with the realisation that a crystal is the supramolecule *par excellence*[16] – held together by hydrogen bonding, electrostatic and van der Waals interactions and metal coordination – came the concept that crystal engineering is the synthesis of supramolecular structures in the solid state. Although the crystal is conceptually an "infinitely" large supermolecule, it (and hence the intermolecular bonding) is reduced to a motif – the repeating 'unit of pattern' of the unit cell – as a result of the conventions of crystallography.[17]

The importance of crystal engineering extends to the possibilities of developing novel industrial heterogeneous catalysts as well as applications in materials science, including storage matrices for gases such as hydrogen and methane, to mention but a few. The study of solid-state structures by means of crystallography can also provide

us with valuable information about solution-phase supermolecules, which can currently only be studied by less precise techniques.[12]

One of the ultimate goals of crystal engineering is to exploit, at will, the connections (*i.e.* intermolecular interactions) that drive supramolecular structure.[18] Different strategies have been developed for the design of molecular crystals (this includes host:guest systems) and one such strategy will be discussed presently. A well-known example of a methodology of this type was developed by Desiraju and co-workers in which supramolecular synthons (or motifs) are used in a supramolecular retrosynthesis, where the crystal becomes the retrosynthetic goal. The term "synthon" refers to substructural units consisting of intermolecular interactions that are identified and used in an analogy to the established concept of covalent retrosynthesis.[19] This is to say that these motifs can be carried over from one crystal structure to another (like covalent reactions), and if substructural units are correctly identified within a target supermolecule, then appropriate precursor molecules should be able to construct that target. In any organic crystal, the intermolecular interactions can be considered as linkages and the molecules as nodes, and subsequently the crystal can be simplified as a network that allows specific synthons needed for one-, two- or three-dimensional architectures to be predicted. Figure 1.2 shows examples of some rudimentary synthons (design elements) where (N,O)–H···O interactions are combined in different ways to yield a series of homodimeric motifs. A more complete set of synthons also includes interactions such as weaker forces and mixtures of interactions.

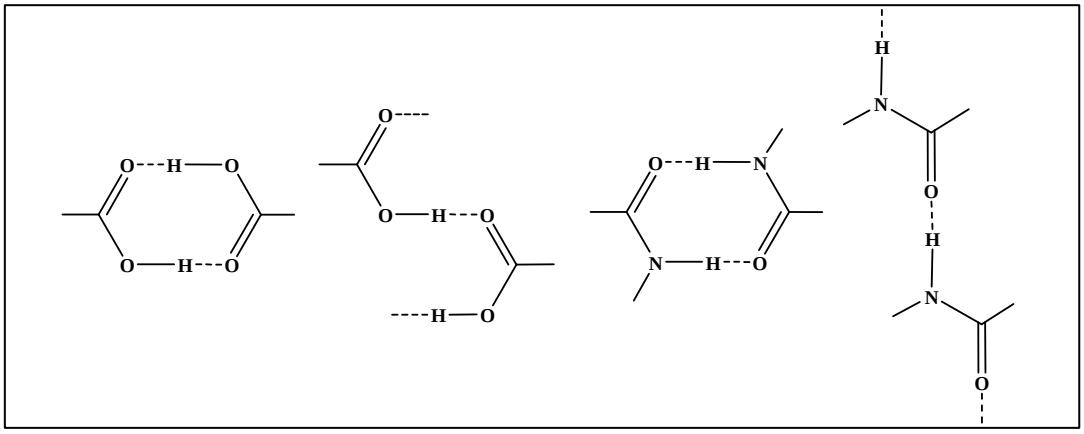

Figure 1.2 Examples of some supramolecular synthons. For a more comprehensive account of supramolecular synthons, the reader should consult a review on the subject by Desiraju.[18]

The earlier work of Etter and co-workers can also be viewed as a form of deconstruction of the crystal and certainly contributed to the later concept of the *synthon*. They studied the topology of hydrogen bonding patterns in the solid state and developed a method for describing hydrogen bonding patterns using symbols (encoding) as well as general rules concerning expected hydrogen bond organisation in organic solid-state structures (decoding).[20,21] The analysis and subsequent symbolic description of hydrogen bonding patterns in this manner is referred to as "graph set analysis" (this was preceded by Kuleshova and Zorkii's graph theory).[22] This can be illustrated using a very elementary example (Figure 1.3): monocarboxylic acid dimers can be represented by a finite dimeric graph, but this pattern is also a recognisable component of the infinite repeating hydrogen bonding pattern of a dicarboxylic acid. Here the repeating hydrogen pattern is termed a motif. Using graph set notation, these motifs can now be denoted as either **C** (chain), **R** (ring), **D** (dimer, or other finite set) or **S** (intramolecular hydrogen bond). By assigning superscripts and subscripts, the number of acceptors (a) and donors (d) in each motif can be indicated along with the size of the motif (number of atoms in the repeat unit) shown in parentheses. Thus, both pattern types shown in Figure 1.3 have a graph set of $\mathbf{R}_2^2\mathbf{(8)}$. For higher order networks, combinations of motifs can be specified

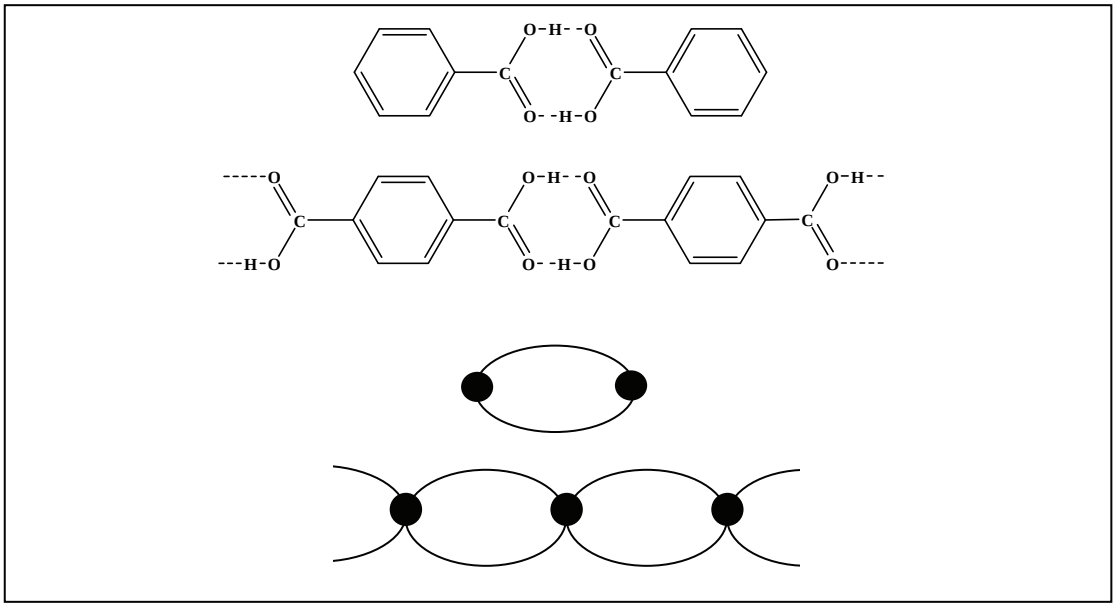

Figure 1.3 Graphs (bottom) representing hydrogen bonding patterns of the monocarboxylic acid dimer and the dicarboxylic acid polymer (top).

independently and, in this regard, the graph set method has proven to be very useful for describing polymorphic relationships.

The importance of understanding the factors governing supramolecular packing was also raised by Schmidt who stated that "… once the solid-state chemist has the tools with which to control molecular packing arrangements, he will be able to follow new lines of experimentation which, so far, have been largely denied to him."[14] The understanding of intermolecular interactions is as important to the crystal engineer as the understanding of the covalent bond is to the synthetic chemist.[23] In light of these statements, it is clear that crystal engineers require a better understanding of intermolecular interactions. Once known, these rules can then be exploited and utilised for the rational design and construction of functional materials (this represents the "why" of crystal engineering).[24] Statistical analyses of many crystal structures are necessary, especially when studying the weaker interactions.[12,25] Records of these interactions are now conveniently available in crystallographic databases such as the user-friendly Cambridge Structural Database (CSD). The CSD[26] also provides software for the search, retrieval and display of structural information and thus affords a vast amount of insight into the intermolecular bond.[27] Recent improvements in crystallographic techniques and computer technology have also facilitated a reduction in time needed for data collection and structure solution, leading to an increasing number of additional structures being deposited with the CSD each year. From the crystal engineer's perspective, the best way to categorise intermolecular interactions is to look at their distance-dependence and directionality. The packing of molecules in the solid state to ultimately form a crystal is governed by two types of interactions (i) medium-range isotropic forces (close-packing, molecular shape and size) typically limited to C···H, C···C and H···H interactions and (ii) long-range electrostatic and anisotropic forces (heteroatom intermolecular interactions) frequently among N, O, S, Cl, Br, I – and between any of these elements and carbon or hydrogen.[12] Essentially, supramolecular construction invokes a balance of all crystal packing forces – a compromise between different strengths, directionalities and distance-dependent characteristics.[28] The chemistry and geometry of intermolecular interactions have also been likened to supramolecular 'glue' or 'cement'.

A short summary of each of the major classes of intermolecular interactions follows.

NONDIRECTIONAL INTERACTIONS

Dispersion forces constitute a major contribution to a crystal's lattice energy and they originate from interactions between fluctuating multipoles in adjacent molecules. These forces are attractive in nature, with an approximately inverse sixth power dependence on the interatomic separation, and a roughly direct dependence on the size of the molecules. Repulsive forces (also referred to as exchange-repulsion forces) stabilise dispersion forces and are inversely related (r^{-12}) to distance. These two nondirectional forces (dispersion and repulsion) are often referred to collectively as van der Waals forces.[12]

Although all atoms in organic molecules may contribute to van der Waals forces, these forces are mostly associated with C···C, C···H and H···H interactions as a result of the relative abundance of these elements in organic systems. Owing to the high ratio of H:C in aliphatic molecules, it is the H···H interactions that are in the majority and these forces are thus significant for longer alkyl chains. Aromatic hydrocarbon molecules possess a cyclic (or polycyclic) framework with π-delocalised electron density, and have a relatively flat local geometry, these molecules also have a higher C:H ratio than aliphatic compounds. As a result of the high C:H ratio, aromatic molecules have a propensity to stack in an effort to maximise the C···C interactions. C···H interactions are also important in some aromatic molecules, and these interactions are optimised by dovetailing of neighbouring molecules in three dimensions. Two extreme geometric relationships between neighbouring aromatic

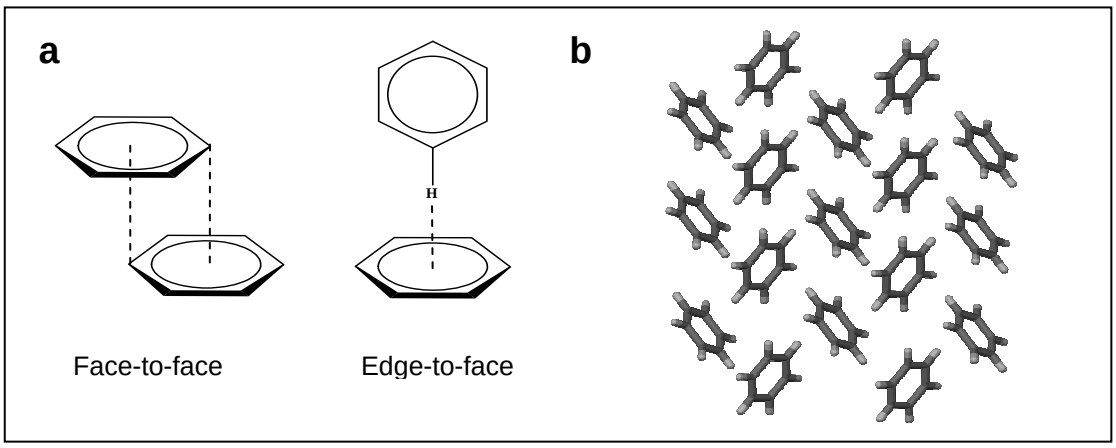

Figure 1.4 **(a)** The two types of π-interactions and **(b)** the herringbone motif often seen for aromatic hydrocarbons as a result of edge-to-face interactions.[9]

molecules can exist: (i) offset-face-to-face (π-stacking) where the C···C interactions dominate and (ii) edge-to-face (T-shaped) where the C···H interactions dominate (Figure 1.4a). A number of intermediate geometries are also known (Figure 1.4b). Intermolecular interactions between aromatic fragments of molecules are frequently encountered in many areas of chemistry and biology,[29] and are of particular importance in the fields of molecular recognition and supramolecular organisation.[30]

According to Hunter and Sanders,[31] aromatic interactions can, in general, be attributed to both electrostatic and van der Waals forces. The electrostatic component, although minor, provides directionality due to maximisation of the electrostatic stabilisation energy. The π-π interactions are not due to attractive forces between π-delocalised systems, but are rather a consequence of the strong attractive interactions that exist between the π-electrons and the σ-framework, and compensate for the π-π electron repulsion contribution.

HYDROGEN BONDING

Hydrogen bonds are considered to be the most important directional interactions in supramolecular construction[18,32] and the literature on the subject dates back to the beginning of the 20th century.[33,34] It is interesting to note that some of the stronger hydrogen bonds are comparable in energy to the weakest covalent bonds, while the weakest hydrogen bonds are similar in energy to van der Waals interactions.[35] Some very well-studied host assemblies that are based on hydrogen bonding include hydroquinone,[36] trimesic acid,[37] Dianin's compound[38] and the ureas.[39] Hydrogen bonds can be represented by the notation D–H···A–X, (D = donor, A = acceptor) and described by the D···A and H···A lengths, the hydrogen bond angle D–H–A or θ, the H–A–X angle or ϕ and the planarity of the DHAX system (Figure 1.5).[15] Although simple hydrogen bonds involve one donor and one acceptor, bifurcated and trifurcated hydrogen bonds, with three and four centres respectively, have also been observed.[40]

Strong hydrogen bonds (O–H···O, O–H···N, N–H···O) with energies of 4-15 kcal.mol^{-1} are mainly electrostatic in nature and, in most cases, donor and acceptor atoms

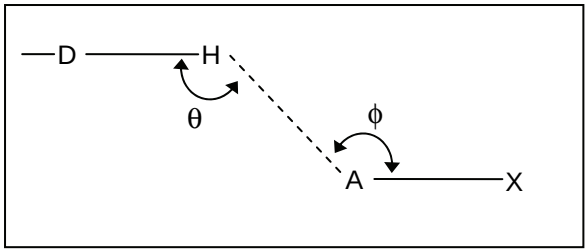

Figure 1.5 The notation commonly used to describe a typical 'simple' hydrogen bond.

experience van der Waals overlap. O···O and N···O (D···A) distances are typically close to 2.75 and 2.85 Å, respectively and deviate from these values only within a narrow range.[25] Where functional groups capable of forming strong hydrogen bonds are present, these bonds will generally form, which makes them valuable components of the crystal engineer's toolkit. Another type of very strong or ionic hydrogen bond also exists (O–H···O$^-$, O$^+$–H···O) with partial covalent character and energies of 15-40 kcal.mol^{-1}. Weak hydrogen bonds (C–H···O, C–H···N and the rare O–H···π, N–H···π)[41-43] with energies of 1-4 kcal.mol^{-1} can be considered to be anything from an electrostatic "bond" to a "bond" barely stronger than a van der Waals interaction.[44] Even though these interactions are low in energy, it has been demonstrated that C–H···O and C–H···N interactions are of importance in a variety of chemical and biological structures.[45] In contrast to the strong hydrogen bonds, these weak interactions are not clear-cut and D···A distances for the C–H···O(N) interaction vary from 3-4 Å. This range of observed "bond" lengths (from 3-4 Å) is not always within the sum of the van der Waals radii, since these interactions have a more electrostatic character where there is only r^{-1} dependence on distance (as opposed to dispersion forces where there is an approximate inverse sixth power dependence on distance).[25] These long range electrostatic forces pose the largest problem to the crystal engineer when considering crystal structure prediction. Where nondirectional forces dominate, close-packed arrangements can be expected. On the other hand, when strong hydrogen bonds come into play (with contributions from other forces being minimal) crystal geometries are often easily understood. However, most structures also involve an assortment of weak directional interactions (such as C–H···O, C–H···N, O–H···π), sometimes displaying more isotropic character, but in other cases (where they are more abundant) directing crystal packing, which makes their effects difficult to predict.[12,28] Robertson express the notion of maximum hydrogen bonding as "…all the available hydrogen atoms attached to electronegative groups are generally

employed in hydrogen bond formation. Some of the bonds formed may be weaker than others, but the molecular packing is generally capable of adjustment in such a way as to permit the fulfilment of this condition."[46]

Other weak interactions which have not been studied in as much depth in terms of host:guest chemistry, and which will not be discussed here, include halogen atom interactions and sulphur atom interactions.[47-49]

THE COORDINATION BOND

A coordination bond is an ion-dipole interaction and normally forms between an acceptor ion and a ligand that donates free electrons. Some well-studied supramolecular assemblies include complexes of alkali metal cations with macrocyclic ethers (termed "crown ethers"), where the oxygen lone pairs are attracted to the cation's positive charge. The coordination bond has some advantages over the other intermolecular bonds, since it is highly directional and much stronger (20-45 $kcal.mol^{-1}$). For exactly this reason, coordination polymers have received much attention lately and this has led to the development of metal-organic framework structures (MOFs). Some aspects of these structures and the use of the coordination bond will be discussed in section 1.4.

MOLECULAR ASSEMBLY

Self-assembly is one of the core concepts of supramolecular chemistry, and has been studied intensively in the context of biological processes. Self-assembly can be defined as the spontaneous construction of high-order structures from molecular building blocks and in this sense is almost synonymous with supramolecular chemistry. In short, self-assembly encompass all the afore-mentioned intermolecular interactions. Our group is interested in the process of self-assembly of molecules from solution or vapour to form crystals. Of course, this concept is also of high relevance to crystal engineers. A prime example of reversible (or strict) self-assembly is that of the tobacco mosaic virus (TMV). The virus particle assembles in a complex process from its constituent coat protein and RNA, and disassembly is achieved by an intricate process initiated by electrostatic interactions.[50,51]

As previously mentioned, crystal engineering has its roots in organic chemistry, but has long since grown to include a number of different areas of research, spanning physical chemistry, crystallography, inorganic chemistry and green chemistry (to mention a few). This is also evidenced by the number of printed works covering the field. For a broader overview the reader is referred to *Crystal Engineering. From Molecules and Crystals to Materials*,[52] *Frontiers in Crystal Engineering*[53] and *Crystal Design. Structure and Function. Perspectives in Supramolecular Chemistry*.[54]

1.3 INCLUSION COMPOUNDS

The discovery of chlorine clathrate hydrate in the early nineteenth century by Humphrey Davy marked the start of the field of host:guest chemistry.[55] More clathrates discovered in the 19th century included hydroquinone inclusion compounds, Hofmann's benzene compound ($Ni(CN)_2 \cdot NH_3 \cdot C_6H_6$), Dianin's compound and other clathrate hydrates (*i.e.* of SO_2, Br_2, CH_4).[56,57] The next notable milestone was the development of X-ray crystallography, which would eventually allow the structural characterisation of these and other inclusion compounds. The first structural elucidation of a host:guest complex was reported by H. M. Powell in 1948.[58] The earliest synthetic host compounds based on molecular recognition followed *ca* two decades later – namely Pedersen's cyclic polyether crown compounds,[59] Park and Simmond's anion hosts[60-62] and the first cryptands by Lehn.[63-67] In the development of host:guest chemistry, and especially supramolecular chemistry, there are three events (or rather key concepts) that need mentioning, although the interdisciplinary field of supramolecular chemistry was only established long afterwards:

1) In 1893 Alfred Werner established his theory of coordination chemistry, where selective binding must involve attraction or mutual affinity between host and guest.[68]

2) In 1894 Emil Fischer introduced the 'lock and key' concept, where the guest has a geometric size or shape complementary to that of the receptor (Figure 1.6).[69]

3) In 1906 Paul Ehrlich realised that molecules do not act if they are not bound, and introduced the concept of a biological receptor (receptor-substrate binding).

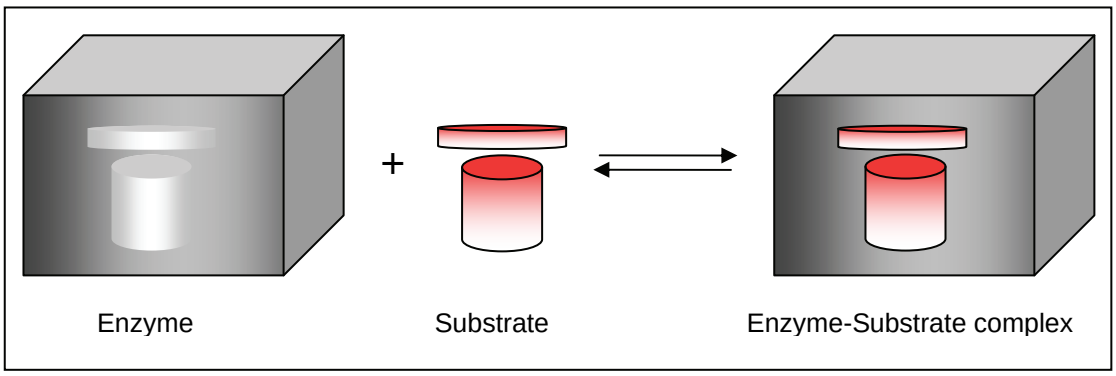

Figure 1.6 Emil Fischer's 'lock and key' concept for enzyme-substrate binding.[9]

In 1977 Cram *et al.* made the following statements about host:guest complexation, which describe the nature of host:guest interactions very well:[70] "Complexes are composed of two or more molecules or ions held together in unique structural relationships by electrostatic forces other than those of full covalent bonds or of ionic crystals ... More specifically, molecular complexes are usually held together by hydrogen bonding, by ion pairing, by π acid to π base interactions, by metal to ligand binding, by van der Waals attractive forces, by solvent reorganising, and by partially made and broken covalent bonds (transition states) … A host:guest relationship involves a complementary stereoelectronic arrangement of binding sites in host and guest. The host component is defined as an organic molecule or ion whose binding sites converge in the complex. The guest component is defined as any molecule or ion whose binding sites diverge in the complex."

It is clear that, when looking at the host:guest chemistry of today, there has been major growth since the first synthetic host compounds and the realisation of the field of supramolecular chemistry. While it started mainly with the design of unimolecular hosts for recognition of specific molecules (*e.g.* cryptates, cyclophanes and crown ethers) in solution, it now stretches into the realms of crystal engineering, where host 'status' is often only relevant in the solid state (multicomponent molecular crystals) and host and guest constituents interact by means of relatively weak interactions.[71,72] In host:guest chemistry, neutral guest species are only weakly associated with the host framework, but inclusion phenomena can nevertheless give rise to many important applications. Some of these potential applications include the resolution of racemates and the separation of mixtures of compounds, the controlled release of pharmacologically active compounds, the enforcement of particular reaction pathways by inclusion of reactants within the confined spaces of the structure (topochemistry), the stabilisation of reactive species and the solid phase storage of gasses and toxic materials.[9]

Considering that host:guest chemistry has developed significantly since Cram's[70] working definition, it has become necessary in 'modern' host:guest chemistry to distinguish between two types of host frameworks.[73] The first type of host is a single molecule with the guest located within its cavity – this category is generally referred to as the cavitands, and guest-binding can occur both in solution and in the solid state

(Figure 1.7a). In the second class, multiple host molecules assemble to form a guest-accessible cavity and the guest is included within this cavity as part of the repeating motif of the crystalline lattice (Figure 1.7b). These materials are referred to as clathrands, and the corresponding host:guest complexes are called clathrates, while the cavitands form cavitates. This section will mainly focus on solid-state clathrates/cavitates of organic hosts. Inorganic materials and coordination compounds will be discussed in more detail in the next section on porosity.

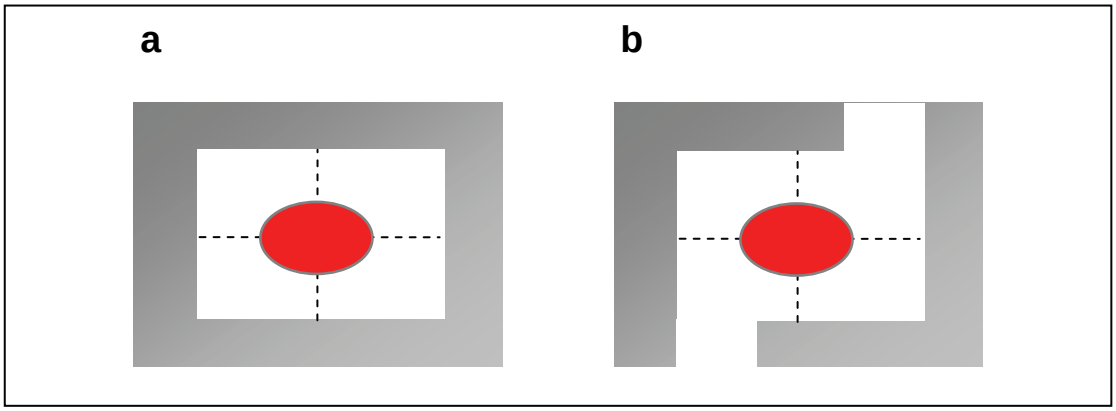

Figure 1.7 A scheme showing the two types of host:guest complexes, **(a)** the guest molecule surrounded by the host and **(b)** a pair of host molecules aggregate to enclose the guest molecule.[12]

Chief among materials already implemented in industrial applications are the more 'conventional' inclusion compounds, such as the zeolites, layered solids and intercalates. Zeolites occur naturally, but synthetic zeolites are also used industrially (notably ZSM-5, which is used in the petrochemical industry for gasoline production).[74] There are a large variety of applications for layered solids and intercalates, ranging from their uses as lubricants (graphites), electrodes for solid state batteries (layered-metal chalcogenides and graphite intercalates) and other battery applications requiring high-energy density such as pacemakers and cell phones (TiS_2), to their use as ion exchange media.[75] Interest in pillared clays (with pore sizes greater than 1 nm) has recently been revived because of their ability to crack heavy oil fractions – this cannot be achieved with zeolites owing to pore size limitations.[9] Clathrate hydrates also have industrial relevance because, in most cases, they are thermally more stable than ice. Because of this property, methane clathrate formation is a significant problem in the drilling and transportation industry. However, the inherent stability of methane clathrates also facilitates the occurrence of large natural gas reserves that can be utilised as a viable source of energy.[76] These applications

illustrate the variety of existing uses of inclusion compounds as well as their industrial relevance. An understanding of their structure is crucial to their being utilised in a beneficial manner, as is a thorough study of the inclusion behaviour of the respective host molecules.

One of the goals of the study of host:guest systems is to design hosts that are able to form robust scaffolds that are unaffected by the choice of guest, and thus also to produce hosts that are able to accommodate an assortment of guests. It is also desirable that designed host molecules have easily tuneable features that will not change the core structure of the host. To date, various host:guest systems have been reported that satisfy these conditions, and a few of these systems will be discussed briefly, along with some strategies for future successful host:guest design. Among these are some examples that reliably form clathrate-type host:guest complexes in the solid state and, as a result of being able to form their clathrate architecture irrespective of the guest species, particular materials have been studied quite extensively. A few classical examples include hydroquinone, urea, tri-*o*-thymotide, cyclotriveratrylene, gossypol, Dianin's compound and perhydrotriphenylene.[77]

When considering these well-studied host systems, some themes for host design become apparent. Close packing of the apohost is the principal problem that the crystal engineer needs to overcome for successful host synthesis. Several creative strategies have been used to circumvent this. One way of achieving this is to use irregularly shaped host molecules that consequently do not have the ability to close-pack well in the solid-state. Inclusion of a second molecule of the appropriate size, shape and functionality may therefore become favourable. An example includes Toda's wheel-and-axle compounds (Figure 1.8), where bulky end groups are added to rigid linear spacer moieties. The diol shown in Figure 1.8a forms crystalline adducts with various guest molecules.[78] Toda's wheel-and-axle concept has since been shown by Hart and others to afford hosts with great potential for versatile inclusion chemistry.[79]

Another class of host compounds (most likely not resulting from a design strategy as their discovery must have been serendipitous) consists of some low-symmetry molecules capable of hydrogen bonding, where the overall symmetry of the host

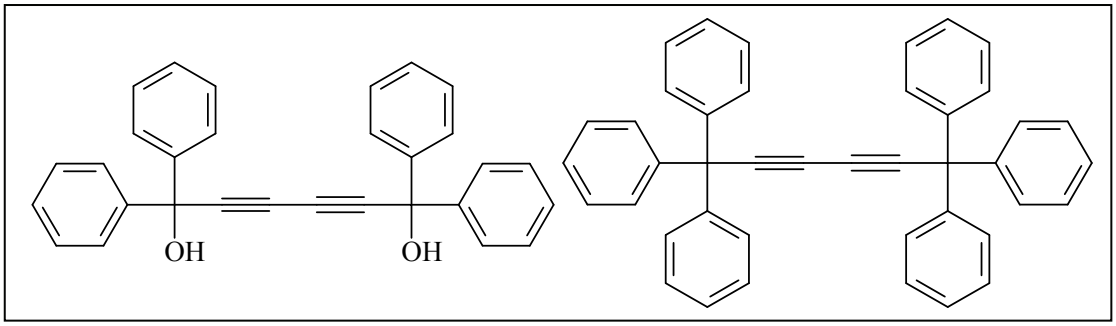

Figure 1.8 1,1,6,6-tetraphenylhexa-2,4-diyne-1,6-diol (left) and 1,1,1,6,6,6-hexaphenylhexa-2,4-diyne (right).

packing is higher than that of the individual host molecules. Most of these molecules have hydrogen bonding groups that are not as geometrically constrained as the carboxylic acids, and this degree of flexibility in the hydrogen bonding patterns as well as in the molecules themselves is expected to play a large role in the formation of very symmetrical supermolecules.[12] Such host structures include the well-studied Dianin's compound,[38,80] Bishop's alicyclic diols[81] and ureas.[82,83] The urea (or thiourea) clathrates are considered to be the most well-known organic system, with *syn* and *anti* N–H···O(S) hydrogen bonds (Figure 1.9) affording double-helical hexagonal channels capable of hosting long-chain hydrocarbons such as *n*-alkanes.[9]

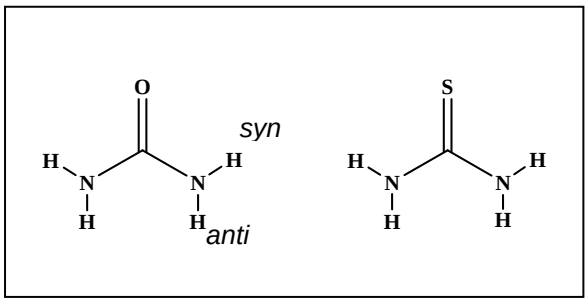

Figure 1.9 Urea (left) and thiourea (right).

Dianin's compound is a member of the "hexahost" family as termed by MacNicol, and other hosts included in this series are phenol and hydroquinone.[36,71] In the solid state, each of these compounds packs to afford six-membered hydrogen bonded rings with the aromatic moieties arranged in an alternating up-down fashion (Figure 1.10a). This arrangement results in a cavity bounded by the aromatic rings and has (in the case of hydroquinone) been shown to include guests even as large as C_{60}.[84] Dianin's compound has proven to be a very versatile host, forming the stable hexagonal ring in the presence of a wide variety of guests and even in the absence of guests. The

Dianin's hexahost design concept has been used extensively – synthetic analogues were first prepared by MacNicol and have been shown to mimic this architecture and display inclusion behaviour. Figure 1.10a shows a typical six-membered hydrogen bonded ring, and Figure 1.10b illustrates replacement of the hydrogen bonded hexagon by an aromatic ring in a hexasubstituted benzene.

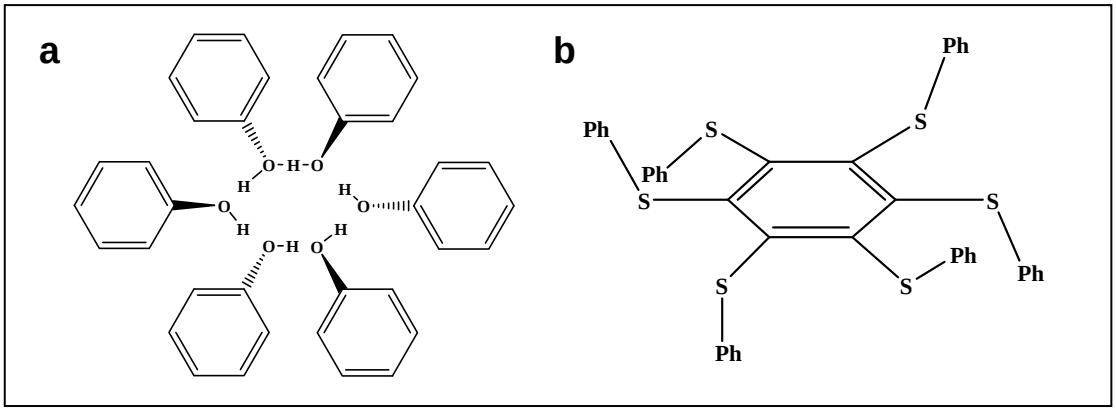

Figure 1.10 **(a)** The well-known hexagonal hydrogen bonded ring with aromatic moieties arranged in an alternating up-down fashion to form a hexahost. **(b)** A molecular analogue where the hydrogen bonded ring has been replaced by a covalent ring in the form of benzene and substituents still adopt an up-down arrangement.[9]

Another class of host compounds can be identified in which the directionality of hydrogen bond moieties is exploited to create a rigid host framework (in such cases

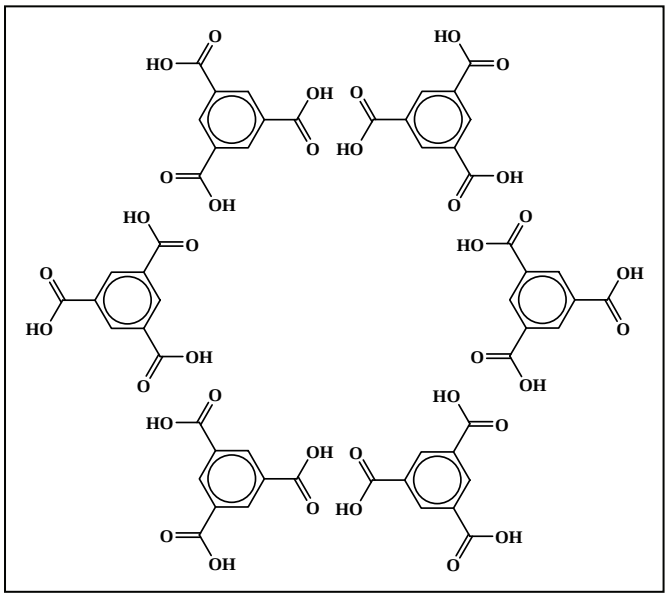

Figure 1.11 The hexagonal arrangement of trimesic acid.

close-packing tendencies can be overcome). Examples are adamantane-1,3,5,7-tetracarboxylic acid and trimesic acid (1,3,5-benzenetricarboxylic acid), which utilise the carboxylic acid dimer synthon and the symmetry of the molecule therefore guarantees an open framework (Figure 1.11).

The use of supramolecular hosts generally does not involve much crystal engineering because, in such cases, the host is structurally predisposed for specific guest binding, which can occur both in solution and in the solid state. Preorganisation make use of the chelate and macrocyclic effects as well as shape and electronic complementarity. Examples of hosts that encapsulate cationic guests include the crown-ethers,[85] spherands[86] and the cryptands.[87] Other hosts that form intracavity complexes with neutral guest molecules include the cavitands, cyclodextrins,[88] cyclophanes,[89] crytophanes,[90] carcerands and hemicarcerands.[91] Two examples of crown ethers are 18-crown-6 and dibenzo-18-crown-6 (Figure 1.12a and b);[59,92] these compounds have been shown to bind both neutral and cationic guests. The very well-known calixarenes[93] (so named because of their characteristic bowl- or calix-like shape, Figure 1.12), are another example of a metacyclophane-type supramolecular host.

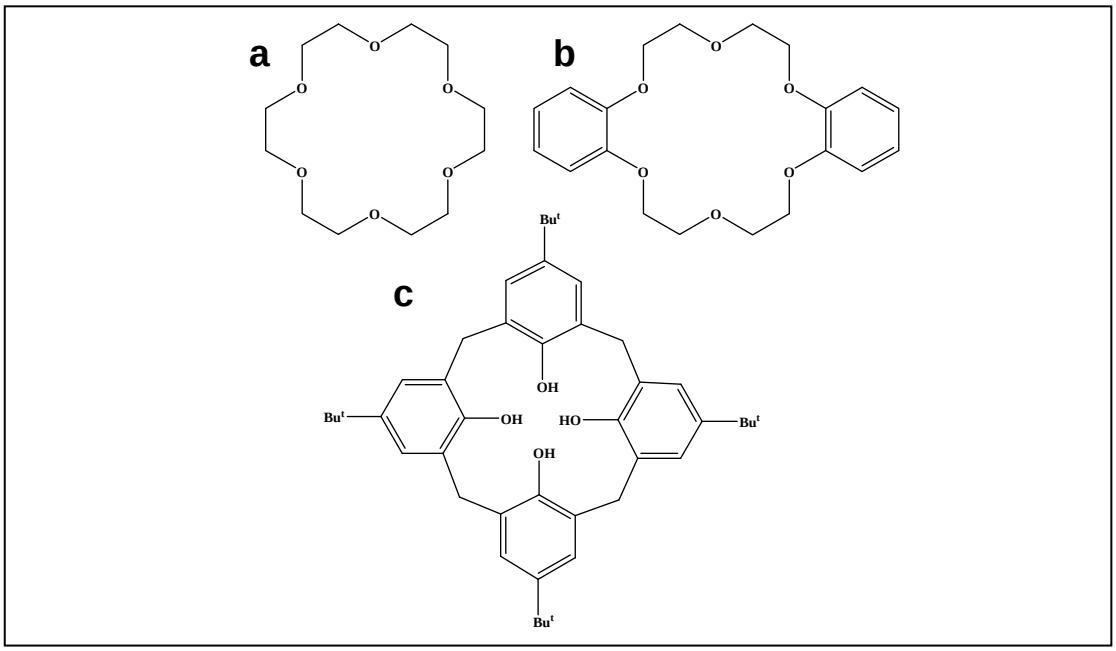

Figure 1.12 **(a)** 18-crown-6 and **(b)** dibenzo-18-crown-6 and **(c)** *p-tert*-butylcalix[4]arene.

The process of guest inclusion by a host can be represented by the following equation:[94]

$$H\,(s,\alpha) + nG\,(l \text{ or } g) \rightarrow H \cdot G_n(s,\beta)$$

where α is the pure phase of the host H, β the phase of the host:guest compound and *n* the host:guest ratio. A scheme illustrating host:guest formation and possible phase changes accompanying guest removal is shown in Figure 1.13.

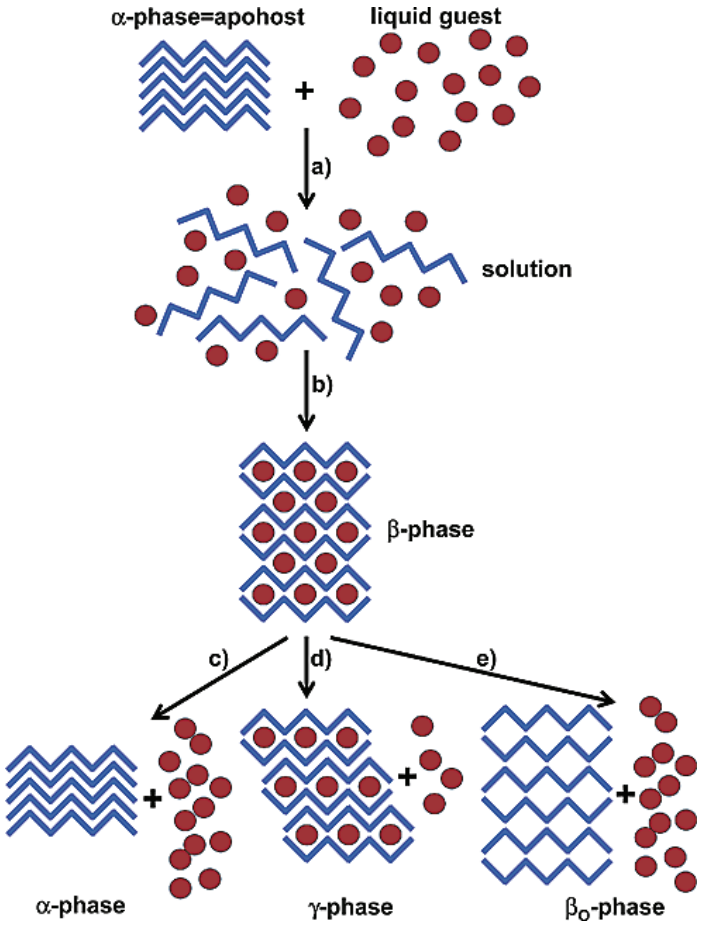

Figure 1.13 Scheme showing possible host:guest formation and decomposition processes. **(a)** Dissolution, **(b)** crystallisation, **(c)** guest removal with collapse of lattice, **(d)** partial guest removal with reorganisation in lattice and **(e)** guest removal without rearrangement of the lattice.[94]

Steps **a** and **b** do not necessarily need to involve dissolution and recrystallisation; for example much success has recently been achieved with methods such as solvent-drop grinding.[95] The β-phase (the inclusion compound) can be analysed with conventional methods such as single-crystal X-ray diffraction (SCD) or X-ray powder diffraction (XRPD), or any other solid-state method as appropriate. The guest removal process

(**c**-**d**) might occur spontaneously, but is often achieved by methods such as heating or placing the sample under vacuum. Characterisation of processes **c**, **d** and **e** can often be problematic because transformation of the β-phase to the α-, γ- or β_o-phases upon guest removal is often accompanied by loss of crystal mosaicity. This generally means that the transformed phase cannot be characterised using SCD, and methods such as XRPD, thermogravimetric analysis (TGA) and differential scanning calorimetry (DSC) need to be used to study the host:guest decomposition process.[96] TGA is used to obtain accurate host:guest ratios and DSC can yield the onset temperature and enthalpy changes of various thermal events such as guest release (if there is a concomitant phase change), polymorphic phase transitions and melting.[94]

In some host:guest systems the single crystals survive removal of the guest molecules either with concomitant rearrangement of host molecules to form a more close-packed structure, or without rearrangement, thus yielding voids at locations previously occupied by guest molecules. When crystals retain sufficient mosaicity for SCD analysis, this process is termed "single-crystal to single-crystal transformation" (SCTSCT) and crystallographic studies of such phenomena can provide useful information about dynamics in the solid state. Even in the event of a large structural change, which presumably subjects the crystal to a significant amount of mechanical stress, some crystals have been observed to maintain their mosaicity.[97] Although rare, more and more SCTSCT's are being reported and these studies will enable crystal engineers to better understand the processes governing molecular cooperativity in crystals.[98,99]

For more general information on inclusion phenomena and host:guest interaction the reader is referred to the following texts: the book series *Inclusion Compounds*[100] and the *Comprehensive Supramolecular Chemistry* encyclopedia.[8]

1.4 POROSITY

The ability of porous materials to adsorb gases was realised in the 18th century when Scheele measured the volumes of various gases that could be adsorbed by charcoal.[101] Until the second half of the 19th century the preparation of porous materials was relatively unscientific. After this the development of highly porous solids began to accelerate, and this work was supported by the growth of the physical sciences.[102] Since then porous solids have been widely applied to separation and purification in industrial processes, especially since the latter half of the 20th century.[103] Many useful techniques have been developed for the characterisation of porous materials and their study has become a diverse area covering many fields including building technology, separation science, catalysis and soil science.[102] There is currently a need for the development of new sorbent materials and this has fuelled the revival of the field of gas sorption and porous materials. Goals for new adsorbents include the storage (controlled uptake/release) of sufficient amounts of methane and hydrogen as potential transportation energy carriers.[104] Methane is the main component of natural gas and, when considering the viability of using CH_4 as relatively clean transportation fuel, it is clear that conventional adsorbents do not possess sufficient CH_4 storage capability.[105] Current methods of hydrogen storage are also insufficient and unsafe.[106]

Conventional porous materials are crystalline or amorphous materials (albeit organic, inorganic or metal-organic compounds) that possess permanent pores through which they reversibly allow the passage of molecules ('pore' is derived from the Greek word 'poros', meaning hole). In 1985 the International Union of Pure and Applied Chemistry (IUPAC)[107,108] recommended that porous solid materials be classified into three categories on the basis of pore diameter: microporous (or nanoporous, but this term does not adhere to IUPAC convention) (<15 Å), mesoporous (15-500 Å) and macroporous (>500 Å).[109]

Porosity, or rather sorption behaviour, is divided into absorption and adsorption. *Absorption* is a process in which one or more substances are incorporated within another, where *adsorption* is the enrichment of one or more components on an interface (surface layer). The distinction is thus clear, adsorption occurs on the surface and absorption penetrates the surface layer and enters the body of the bulk

solid. Further distinction should be made between two adsorption processes on the basis of the strength and type of interactions, namely physical adsorption (*physisorption*) and chemical adsorption (*chemisorption*). *Chemisorption* normally occurs with the formation of significant chemical bonds and the enthalpy of adsorption is in the range of *ca* 25 – 95 kcal.mol^{-1}. *Physisorption,* on the other hand, occurs when a gas (the *adsorptive*) makes contact with the surface of a solid (the *adsorbent*) and the interaction between *adsorbent* and *adsorbate*[*] is much weaker, consisting of long range electrostatic and van der Waals interactions with the corresponding enthalpy of adsorption being less than *ca* 10 kcal.mol^{-1}. In some cases the distinction between ad- and absorption is somewhat blurred and the term *sorption* is used in conjunction with the general terms *sorbent*, *sorbate* and *sorptive*.[107,110]

The adsorption isotherm is used to denote the adsorption and desorption of a gas on a solid at constant temperature and relates the amount of gas adsorbed (in moles, grams, cm^3 etc.) to the equilibrium pressure of the gas. When adsorption and desorption curves do not match, the process is said to exhibit hysteresis. IUPAC recommends that the adsorption isotherms be plotted with amount adsorbed (preferably in mol of gas per gram of adsorbent) against the relative equilibrium pressure (p/p^o), where p^o the saturation pressure of the adsorptive at the temperature of the specific isotherm. According to IUPAC, which formalised the BDDT convention previously proposed by Brunauer *et al.*,[111] experimentally obtained adsorption isotherms (from physisorption) can be classified into six types (Figure 1.14).[107] The *Type I* isotherm is reversible, with a concave shape, and this behaviour is expected for microporous materials with relatively small external surfaces such as the zeolites and activated carbons. These are often also referred to as Langmuir isotherms. *Type II* isotherms (also reversible) are typically observed for non-porous and macroporous adsorbents and represent monolayer-multilayer adsorption. *Type III* (also reversible) displays a convex shape and is a very uncommon isotherm in which the adsorbate-adsorbent interactions play a significant role. *Type IV* isotherms display hysteresis associated with capillary condensation in mesoporous materials while the initial curvature (similar to type II) is attributed to monolayer-multilayer adsorption. *Type V* is another uncommon isotherm and is obtained for porous adsorbents where the adsorbent-adsorbate interaction is of a weak nature. Type VI isotherms are observed for uniform

[*] The distinction here between *adsorptive* and *adsorbate* is that the adsorptive is capable of being adsorbed and adsorbate is material already in the adsorbed state.

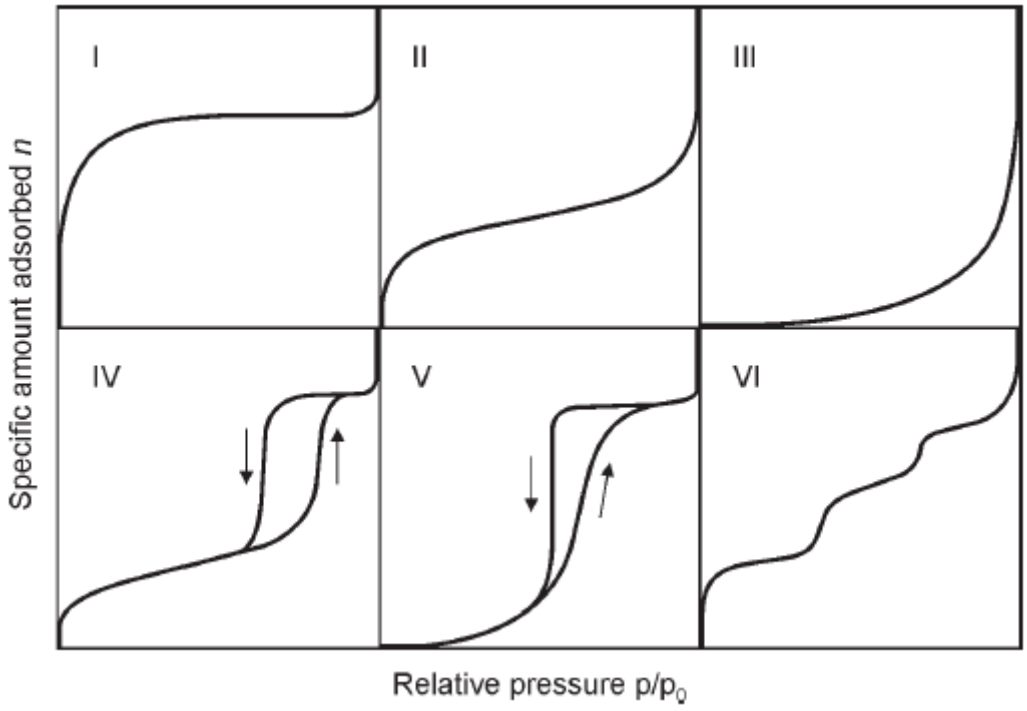

Figure 1.14 Idealised sorption isotherms for type I-VI isotherms as classified by IUPAC.[107]

non-porous surfaces and the steps in the isotherm curve represent step-wise multilayer adsorption.[107]

Since this thesis focuses mainly on microporous materials, and thus materials that display Type I sorption behaviour, more specific details will now be given about such systems. In microporous adsorbents the mechanism of physisorption is slightly different from that in meso- and macroporous sorbents as a result of the molecular-scale dimensions of the pores. These size constraints lead to an increase in the strength of adsorbent-adsorbate interactions, which means that pores become filled with physisorbed molecules at low p/p^o values (see curve I in Figure 1.14).

Many different procedures have been devised to determine the amount of gas adsorbed. Reliable and accurate adsorption data are needed over large temperature and pressure ranges when developing porous materials for industrial applications.[112] Methods currently used are either based on gas flow (here a carrier gas can introduce an adsorptive),[113] volumetric methods (an indirect method based on the determination of the amount of gas removed from the gas phase) or gravimetric methods (a direct method based on the measurement of the weight of the adsorbent). Volumetric and

gravimetric methods of determining adsorption isotherms will be discussed further in the experimental sections 2.5 and 2.6.

The porous materials used in industrial processes have thus far included zeolites (termed 'molecular sieves'), intercalates and layered structures and some amorphous materials. Until the early 1990s (before the study of porosity in the context of crystal engineering) there were only two main types of porous materials: inorganic materials and carbon-based materials. There are two major subcategories in the area of microporous inorganic materials: the aluminosilicates and the aluminophosphates. The well-known zeolites, discovered over a century ago, are three-dimensional crystalline porous materials and comprise the bulk of the framework silicates.[114,115] Zeolites have the general formula $M_{x/n}[(AlO_2)_x(SiO_2)_y]\cdot wH_2O$ where M (an alkaline or alkaline-earth metal) or organic cations balance the charge of the anionic framework and are included in the interstices of the framework built from corner-sharing TO_4 (SiO_4 or AlO_4^-) tetrahedra (T can also include other ions capable of tetrahedral coordination, *i.e.* Ge^{4+}, Ga^{2+}, P^{5+} etc.).[116] The microporous character of zeolites, and their uniform pore dimensions,[117] have provided them with properties of significant industrial interest: their ability to adsorb and separate gases, vapours and

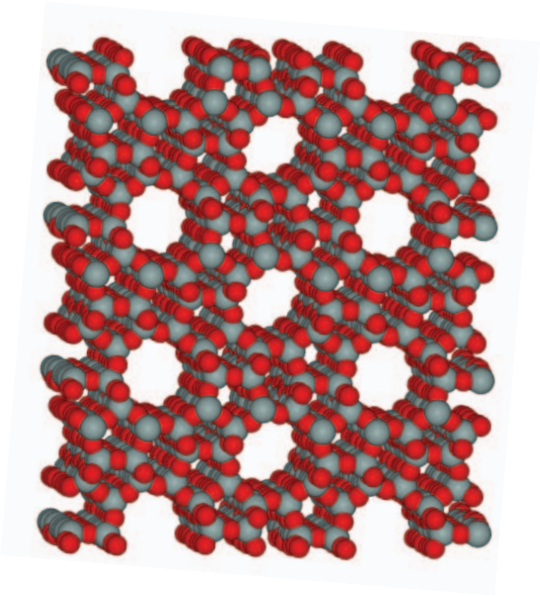

Figure 1.15 A diagram of ZSM-5 shows the TO_4 tetrahedra and linear channels. Linear channels also propagate perpendicular to those shown in the figure and the channels interconnect in a zig-zag fashion.

liquids; their success in a wide variety of catalytic reactions; and their ability to act as ion exchangers.[9,103] For instance, ZSM-5[74,118] (a synthetic zeolite) is used in the synthesis and separation of *p*-xylene from the *m*- and *o*-isomers, and is also used in the synthesis of branched alkanes from *n*-alkanes (petrochemical cracking). The topology of ZSM-5 is shown in Figure 1.15. Although zeolites have proven to be very useful in a range of processes, they possess low porosity and, with current synthetic methods, fine-tuning of the frameworks is not easy.[115]

The layered structures and intercalates are another important group of porous materials that posses micro- and mesoporosity. They include graphite intercalates, clays, hydroxides, phosphates etc. These materials are generally very flexible and can include ionic or neutral guest species. The last group of important porous materials are the amorphous materials. They mostly possess microporosity and include activated carbon, silica gel, activated alumina, gels and colloids and composite materials.[103]

Utilising crystal engineering for the design of porous crystals marked the beginning of a new era in the study of porous materials. Porous crystalline sorbents differ from most of the afore-mentioned materials in that the conventional sorbents (with the notable exception of zeolites) generally exhibit a wide distribution of pore sizes, whereas the pore sizes in crystals are all similar with diameters of molecular dimensions.[119] Molecules in crystals tend to minimise the empty spaces between them (nature abhors a vacuum) in an effort to maximise intermolecular interactions. Therefore it is uncommon to find molecular crystals with open channels or with discrete lattice voids larger than about 25Å^3.[120,121] Consequently molecular crystals have been neglected as porous materials. However, with the growth of crystal engineering the possibility of engineering 'empty' crystals has become a reality and a variety of design approaches have been established. Porous crystalline materials offer an advantage over non-crystalline samples, in that they can be studied using X-ray diffraction methods. Diffraction analysis is a very powerful analytical tool for studying host:guest interactions and, in special cases where solid:gas interactions are being investigated, atomic coordinates of guests can even be determined. If the crystal engineer can obtain more information on gas:solid interactions, the

mechanisms of gas sorption will become clearer and the design of functional materials feasible.

Three classes of crystalline porous materials will now be discussed: 1) rigid metal-organic frameworks, 2) flexible frameworks and 3) seemingly nonporous materials.

Coordination polymers have long received attention as a result of their extreme chemical versatility.[122] Indeed, the phrase "coordination polymers" dates back to the early 1960s with the first review appearing in the mid 1960s.[115,123] The reversible sorption behaviour of coordination polymers have long been reported, *e.g.* Werner complexes,[57,124] Prussian blue compounds,[125,126] Hofmann clathrates[127] and, of course, zeolites.[116,117] A new class of crystalline coordination compounds for porous applications came to the fore almost two decades ago. These are referred to as metal-organic frameworks (MOFs) or hybrid materials. These materials are highly regular (crystalline), can have high porosity and the frameworks result from self-assembly. The coordination bonds (dative bonding of a metal ion and a ligand) have strong directionality and this can be exploited by crystal engineers to provide a significant level of framework design. Indeed a large proportion of coordination polymers have topologies reminiscent of the zeolites, where inorganic octahedral or tetrahedral centres are linked by organic moieties. This concept was introduced by Hoskins and Robson[128,129] and, in their first attempt, they substituted the acetonitrile ligands in $Cu(I)(CH_3CN)_4^+$ by 4,4′,4″,4‴-tetracyanotetraphenylmethane. The result was an infinite diamondoid framework and they estimated that the framework itself only occupies a third of the crystal volume, and that each cavity is about 700 $Å^3$ in size (Figure 1.16). Since then Yaghi and others have built many networks based on this type of topology. They used inorganic or organic secondary building units (SBU's) of octahedra or tetrahedra (and many other geometries) and have named this approach 'reticular synthesis'.[130-132] Examples of three commonly recurring inorganic SBU's are given in Figure 1.17, along with the structure of the well-known MOF-5 reported by Yaghi.[133,134] Reticular synthesis is used to build very rigid three dimensional networks (such as in zeolites) and to produce pore windows leading into large cavities. These materials offer novel applications in catalysis as a result of a greater concentration of active sites, as well as applications in gas sorption and separation.

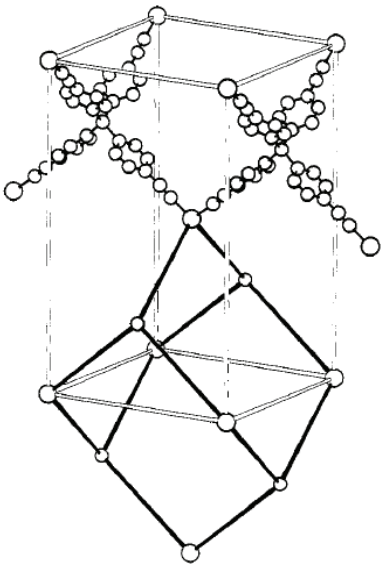

Figure 1.16 The structure of the $Cu^{I}[C(C_6H_4CN)_4]_n^{n+}$ framework.[128]

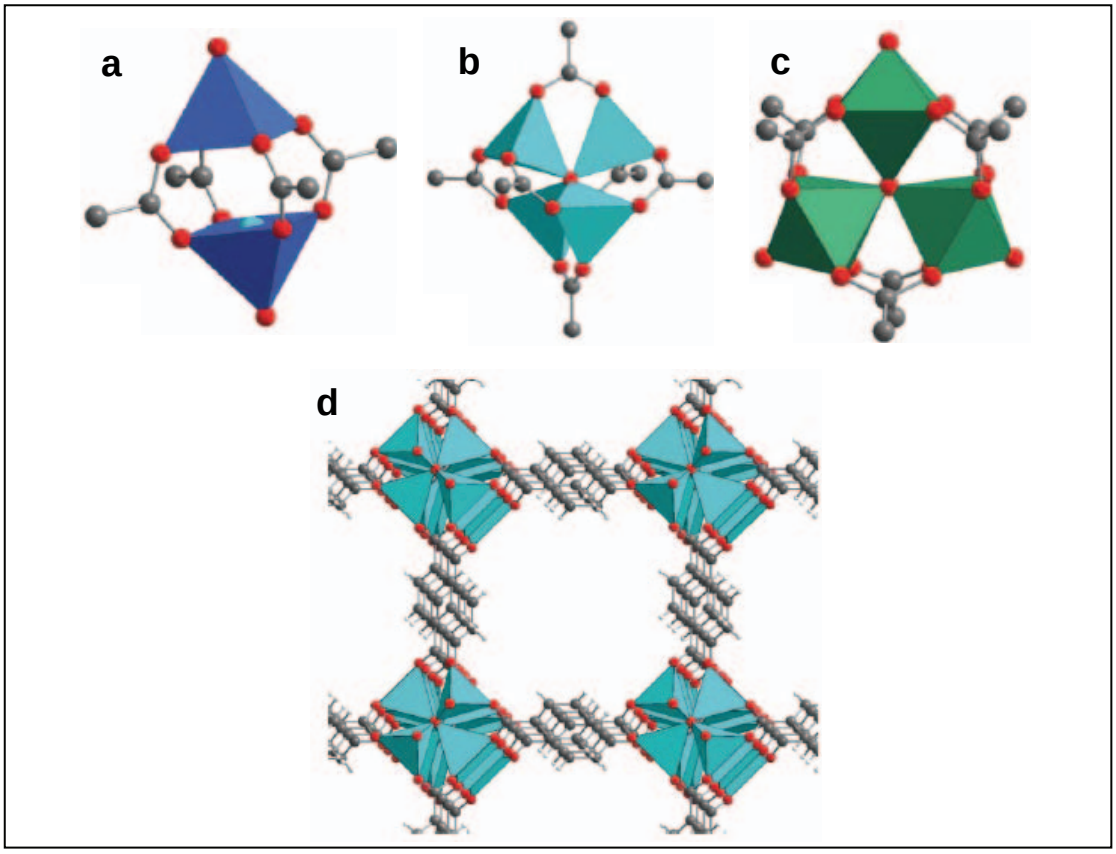

Figure 1.17 **(a)** A "paddlewheel" dimer of CuO_5 square pyramids to form a square SBU. **(b)** The ZnO_4 tetrahedra sharing an oxygen and six carboxylate C atoms to make an octahedral SBU. **(c)** The trigonal planar trimer of CrO_6 octahedra also shares a central oxygen atom and six carboxylates on the periphery. **(d)** MOF-5 is constructed from the octahedral SBU shown in (b) linked by benzene moieties. Carbon and oxygen atoms are shown as grey and red spheres respectively, while CuO_5, ZnO_4 and CrO_6 polyhedra are shown in blue, turquoise and green, respectively.[131,133]

Other accounts of porosity in crystals have brought to light another class of coordination polymers that are related to, but slightly different from the robust MOFs and zeolites – namely *flexible* coordination compounds. The difference is that, in the rigid pore systems, strong coordination and/or covalent bonds form three dimensional networks, whereas in the less-rigid "soft" networks, flexible structural building units are included.[115] More and more reports are being seen of discrete coordination compounds[98] and coordination polymers[135-139] with flexible and dynamic frameworks based on weak intermolecular interactions, and reports also exist of these phenomena in flexible organic frameworks.[71,140-143] Férey and co-workers presented a flexible porous carboxylate (MIL-53)[144] that is built from infinite chains of corner-sharing $MO_4(OH)_2$ octahedra (M = Cr^{3+}, Al^{3+}, Fe^{3+}) interconnected by benzene dicarboxylate units. The resulting three dimensional framework has one dimensional diamond-shaped channels that exhibit a "breathing" behaviour upon hydration and dehydration (Figure 1.18).[145] Apart from the properties that materials with rigid pores exhibit, such as catalysis and gas storage, flexible porous systems can also find applications in molecular sensing, non-linear optical properties and magnetism, to name a few.

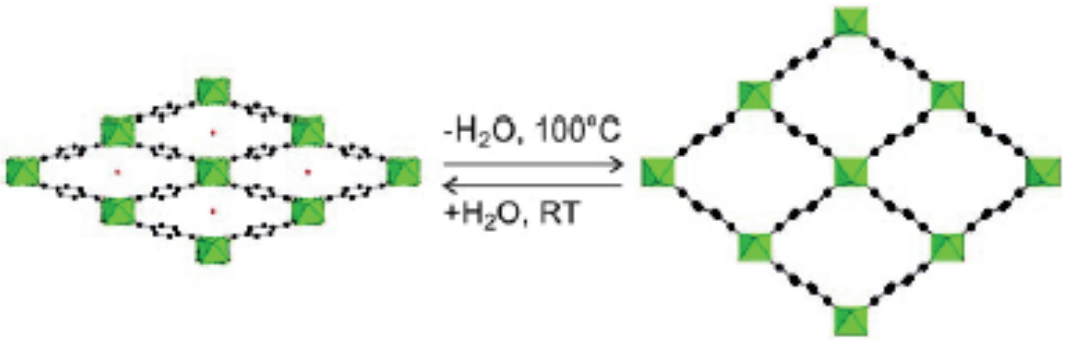

Figure 1.18 The hydration-dehydration process of MIL-53 in which water can be removed to afford a structure with more "open" porosity.[145]

The two classes of coordination compounds discussed so far both exhibit conventional porosity. Before moving on to the final class of porous materials it is useful to discuss the concept of porosity. Conventional porosity, as encountered in 'traditional' porous materials, has already been discussed but any discussion of the porosity in molecular crystals requires further consideration of the concepts involved. According to a recent paper by Barbour,[121] porosity in the literature can be classified into three categories: "conventional porosity, porosity without pores and virtual porosity." Before we look

at definitions of these types of porosity, we should consider the guidelines for the identification of crystal porosity as proposed by Barbour (these have also been suggested by Kitagawa and Yaghi)[131,146]: (1) Evidence should exist that the system is permeable (porous) to species (*i.e.* sorption isotherms, etc.) and (2) when the term "porous" is used, it should be in conjunction with a specific phase of the host and *in principle* the host should be left unaffected by guest uptake/removal. In short, *virtual* porosity most often involves the deletion of selected atoms from a file containing the asymmetric unit of a crystal structure, in most cases the deleted atoms will be small counter ions, solvent molecules and in some cases even ligands bridging two metal ions.

Porosity *without pores* (or virtual porosity) is a relatively new category of porosity, and of particular relevance to this work. It has been reported that crystals (both of organic and coordination compounds) possessing lattice voids, but no atomic-scale channels leading to these voids, can still be permeable to guests.[147] An example is the sublimed *p-tert*-butylcalix[4]arene that crystallises in a low density form with discrete lattice voids of *ca* 235 $Å^3$. These discrete voids cannot be linked by channels according to the crystal structure (*i.e.* using the equilibrium atomic coordinates), but when the crystals are exposed to liquid vinyl bromide a SCTSCT occurs during which vinyl bromide molecules become trapped in the lattice.[148,149] Takamizawa reported a similar phenomenon where a "closed-pore crystal" (assembled from a one dimensional coordination polymer forming discrete cavities) has the ability to absorb carbon dioxide.[150] Various other reports of gas sorption by conventionally 'nonporous' phases of calix[4]arene have also been published by Atwood *et al*.[151-154]

Materials mentioned in these examples do not adhere to the conventional classification of porosity since no permanent porosity is evident. Instead, dynamic porosity exists where the motion of the guest molecules through the crystal occurs by virtue of thermal motion or guest-induced motion of the host molecules. Using atomic coordinates derived from SCD, no channel can be mapped through the crystal; only discrete voids exist that interconnect fleetingly to permit the transfer of guests between neighbouring cavities.

1.5 THESIS OUTLINE

The main objective of this study is to explore some crystal engineering aspects of porous materials based on molecular crystals. The first part of the study concerns itself with the modification of a known organic host compound, while the second part describes three new porous molecular crystals based on coordination compounds.

The experimental techniques and instrumentation used during this study are described in *Chapter 2*.

Chapter 3 discusses the crystal engineering of a known organic host system (Dianin's compound or DC) by synthetic modification. Racemic DC (Figure 1.19a) crystallises with six phenolic moieties forming a hydrogen bonded ring. In this study the aim was to exchange the hydroxyl moiety in one enantiomer with a thiol group (Figure 1.19b). This was done in an effort to investigate if the familiar clathrate architecture would still be obtained if one hydroxyl enantiomer is substituted with its sulphur-analogue, and to see if the pore size of the material could thus be tailored by the altered hydrogen bonding. In this quest to engineer a new porous material, crystallisation of one enantiomer of DC with the opposite thiol-enantiomer led to the assembly of a noncentrosymmetric host:guest adduct. This newly-formed clathrate (which now has an ···O–H···S–H···O–H··· hydrogen bonded ring) is chiral and was shown to order carbon tetrachloride guest molecules in the one dimensional channels (in contrast to what occurs in the racemic DC and thiol-DC clathrates). The carbon tetrachloride inclusion compound also displayed nonlinear optical activity. The chapter is concluded by a study of the desorption and concomitant phase changes of the hybrid OH/SH and racemic thiol-DC carbon tetrachloride inclusion compounds.

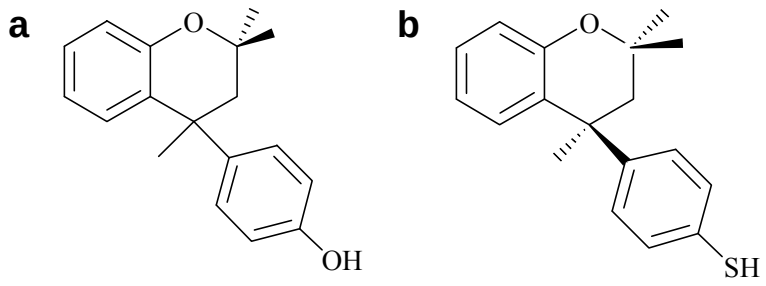

Figure 1.19 **(a)** Hydroxyphenyl-2,2,4-trimethylchroman and **(b)** (*S*)-4-*p*-Mercaptophenyl-2,2,4-trimethylchroman.

The self-assembly of a series of discrete metallocycles from a new imidazole-derived bidentate ligand is reported in *Chapter 4*. The ligand was chosen according to our design strategy of using doughnut-shaped molecules that tend to include solvent in their "holes" as a result of their lack of self-complementarity, which prevents close-packing. Details of the synthesis and structures of five such metallocycles are given, showing them to each be comprised of two ligands coordinated to two metal ions in a cyclic arrangement that include solvent in their as-synthesised forms (Figure 1.20). The desolvation and thermal decomposition are commented on, with reference to TGA, DSC and structural analysis. Two metallocycles are shown to undergo ligand rearrangement on desolvation, while the other three metallocycles produce potentially porous β_o-phases. The three porous metallocycles are isostructural and the only distinction between them is the nature of the anion (Cl^-, Br^-, I^-). The differences in their gas sorption behaviours are also discussed on the basis of their structures. During the course of this study, a miniature pressure cell was developed for routine single-crystal X-ray data analysis under controlled atmospheres of gas. By utilising this device, structural changes are described as a function of increasing gas pressure for one of the porous metallocycles. In this study, two gasses of similar size and geometry, but inverse electrostatic profile were chosen (*i.e.* carbon dioxide and acetylene). Aspects that were investigated and are discussed include the difference in sorption profiles, the difference in host:guest binding (as determined from single-crystal structure elucidation) and statistical mechanics calculations.

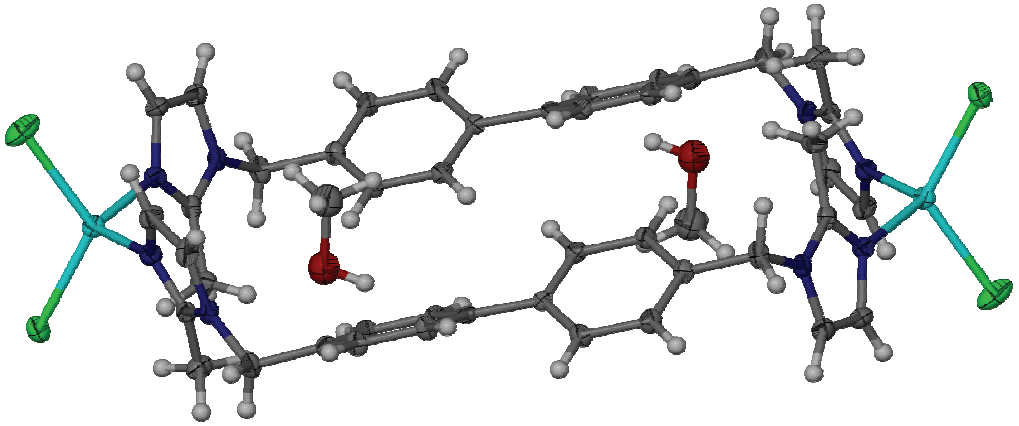

Figure 1.20 The $[M_2\mathbf{L}_2Cl_4]\cdot 2CH_3OH$ metallocycle.

Chapter 5 presents a summary and general conclusions on the work described in Chapters 3 and 4.

REFERENCES

1 J.-M. Lehn, *Angew. Chem. Int. Ed.* **1988**, *27*, 89-112.

2 K. L. Wolf, H. Frahm, H. Harms, *Z. physik. Chem.* **1937**, *B36*, 237-287.

3 K. L. Wolf, H. Dunken, K. Merkel, *Z. physik. Chem.* **1940**, *B46*, 287-312.

4 K. L. Wolf, R. Wolff, *Angew. Chem.* **1949**, *61*, 191-201.

5 J. M. Lehn, *Acc. Chem. Res.* **1978**, *11*, 49-57.

6 J.-M. Lehn, *Pure Appl. Chem.* **1978**, *50*, 871-892.

7 D. Braga, *Chem. Commun.* **2003**, 2751-2754.

8 in *Comprehensive Supramolecular Chemistry*, 1 ed. (Eds.: J. L. Atwood, J. E. D. Davies, D. D. MacNicol, F. Vögtle), Pergamon, Oxford, **1996**.

9 J. W. Steed, J. L. Atwood, *Supramolecular Chemistry*, John Wiley & Sons, Ltd, West Sussex, **2000**.

10 in *Encyclopedia of Supramolecular Chemistry*, 1 ed. (Eds.: J. L. Atwood, J. W. Steed), Marcel Dekker, Inc., New York, **2004**.

11 J. M. Lehn, *Angew. Chem. Int. Ed. Engl.* **1990**, *29*, 1304-1319.

12 G. R. Desiraju, in *Comprehensive Supramolecular Chemistry, Vol. 6*, 1 ed. (Eds.: J. L. Atwood, J. E. D. Davies, D. D. MacNicol, F. Vögtle), Pergamon, Oxford, **1996**, pp. 1-22.

13 R. Pepinsky, *Phys. Rev.* **1955**, *100*, 971.

14 G. M. J. Schmidt, *Pure Appl. Chem.* **1971**, *27*, 647.

15 G. R. Desiraju, *Crystal Engineering, the Design of Organic Solids*, Elsevier, Amsterdam, **1989**.

16 J. D. Dunitz, *Pure Appl. Chem.* **1991**, *63*, 177-185.

17 C. Hammond, *The basics of crystallography and diffraction, Vol. 3*, Oxford University Press Inc., New York, **1997**.

18 G. R. Desiraju, *Angew. Chem. Int. Ed. Engl.* **1995**, *34*, 2311-2327.

19 E. J. Corey, *Chem. Soc. Rev.* **1988**, *17*, 111-133.

20 M. C. Etter, *Acc. Chem. Res.* **1990**, *23*, 120-126.

21 M. C. Etter, J. C. Macdonald, J. Bernstein, *Acta Crystallogr., Sect. B: Struct. Sci.* **1990**, *46*, 256-262.

22 L. N. Kuleshova, P. M. Zorky, *Acta Crystallogr., Sect. B: Struct. Sci.* **1980**, *36*, 2113-2115.

23 J.-M. Lehn, *Angew. Chem. Int. Ed.* **1990**, *29*, 1304-1319.

24 G. R. Desiraju, *Angew. Chem. Int. Ed.* **2007**, *46*, 8342-8356.

25 G. R. Desiraju, *Acc. Chem. Res.* **1991**, *24*, 290-296.

26 F. H. Allen, J. E. Davies, J. J. Galloy, O. Johnson, O. Kennard, C. F. Macrae, E. M. Mitchell, G. F. Mitchell, J. M. Smith, D. G. Watson, *J. Chem. Inf. Comput. Sci.* **1991**, *31*, 187-204.

27 F. H. Allen, O. Kennard, R. Taylor, *Acc. Chem. Res.* **1983**, *16*, 146-153.

28 C. V. K. Sharma, K. Panneerselvam, T. Pilati, G. R. Desiraju, *J. Chem. Soc., Perkin Trans. 2* **1993**, 2209-2216.

29 J. D. Watson, F. H. C. Crick, *Nature* **1953**, *4356*, 737-738.

30 G. R. Desiraju, A. Gavezzotti, *J. Chem. Soc., Chem. Commun.* **1989**, 621-623.

31 C. A. Hunter, J. K. M. Sanders, *J. Am. Chem. Soc.* **1990**, *112*, 5525-5534.

32 T. Steiner, *Angew. Chem. Int. Ed.* **2002**, *41*, 48-76.

33 W. M. Latimer, W. H. Rodebush, *J. Am. Chem. Soc.* **1920**, *42*, 1419-1433.

34 L. Pauling, *The Nature of the Chemical Bond and the Structure of Molecules and Crystals An Introduction to Modern Structural Chemistry*, 2nd ed., Oxford University Press, London, **1940**.

35 R. Yamdagni, P. Kebarle, *J. Am. Chem. Soc.* **1971**, *93*, 7139-7143.

36 T. C. W. Mak, B. R. F. Bracke, in *Comprehensive Supramolecular Chemistry, Vol. 6* (Eds.: J. L. Atwood, J. E. D. Davies, D. D. MacNicol, F. Vögtle), Pergamon, Oxford, **1996**, pp. 23-37.

37 F. H. Herbstein, in *Comprehensive Supramolecular Chemistry, Vol. 6* (Eds.: J. L. Atwood, J. E. D. Davies, D. D. MacNicol, F. Vögtle), Pergamon, Oxford, **1996**, pp. 61-83.

38 P. Finocchiaro, S. Failla, in *Comprehensive Supramolecular Chemistry, Vol. 6*, 1 ed. (Eds.: J. L. Atwood, J. E. D. Davies, D. D. MacNicol, F. Vögtle), Pergamon, Oxford, **1996**, pp. 593-642.

39 M. D. Hollingsworth, K. D. M. Harris, in *Comprehensive Supramolecular Chemistry, Vol. 6* (Eds.: J. L. Atwood, J. E. D. Davies, D. D. MacNicol, F. Vögtle), Pergamon, Oxford, **1996**, pp. 177-237.

40 C. B. Aakeroy, K. R. Seddon, *Chem. Soc. Rev.* **1993**, *22*, 397-407.

41 R. Taylor, O. Kennard, *J. Am. Chem. Soc.* **1982**, *104*, 5063-5070.

42 L. R. Hanton, C. A. Hunter, D. H. Purvis, *J. Chem. Soc., Chem. Commun.* **1992**, 1134-1136.

43 M. A. Viswamitra, R. Radhakrishnan, J. Bandekar, G. R. Desiraju, *J. Am. Chem. Soc.* **1993**, *115*, 4868-4869.

44 G. R. Desiraju, in *Encyclopedia of Supramolecular Chemistry, Vol. 1*, 1 ed. (Eds.: J. L. Atwood, J. W. Steed), Marcel Dekker, Inc., New York, **2004**, pp. 658-665.

45 G. A. Jeffrey, W. Saenger, *Hydrogen Bonding in Biological Structures*, Springer, Berlin, **1991**.

46 J. M. Robertson, *Organic Crystals and Molecules*, Cornell University Press, Ithaca, **1953**.

47 G. R. Desiraju, V. Nalini, *J. Mater. Chem.* **1991**, *1*, 201-203.

48 J. Sarma, G. R. Desiraju, *Acc. Chem. Res.* **1986**, *19*, 222-228.

49 O. Navon, J. Bernstein, V. Khodorkovsky, *Angew. Chem. Int. Ed. Engl.* **1997**, *36*, 601-603.

50 A. Klug, *Philos. Trans. R. Soc. London, Ser. B* **1999**, *354*, 531-535.

51 G. Stubbs, *Philos. Trans. R. Soc. London, Ser. B* **1999**, *354*, 551-557.

52 D. Braga, F. Grepioni, A. G. Orpen, *Crystal Engineering from Molecules and Crystals to Materials*, Kluwer, Dordrecht, **1999**.

53 E. R. Tiekink, J. J. Vittal, in *Frontiers in Crystal Engineering*, Wiley, Chichester, **2005**.

54 G. R. Desiraju, Wiley, Chichester, **2003**.

55 H. Davy, *Philos. Trans. R, Soc. London* **1811**, *101*, 155.

56 B. H. Davis, K. S. W. Sing, *Handbook of Porous Solids, Vol. 2*, Wiley, Weinheim, **2002**.

57 J. Lipkowski, in *Comprehensive Supramolecular Chemistry, Vol. 6* (Eds.: J. L. Atwood, J. E. D. Davies, D. D. MacNicol, F. Vögtle), Pergamon, Oxford, **1996**, pp. 691-714.

58 H. M. Powell, *J. Chem. Soc.* **1948**, 61.

59 C. J. Pedersen, *J. Am. Chem. Soc.* **1967**, *89*, 2495-2496.

60 H. E. Simmons, C. H. Park, *J. Am. Chem. Soc.* **1968**, *90*, 2428-2429.

61 C. H. Park, H. E. Simmons, *J. Am. Chem. Soc.* **1968**, *90*, 2429-2431.

62 C. H. Park, H. E. Simmons, *J. Am. Chem. Soc.* **1968**, *90*, 2431-2432.

63 J. M. Lehn, J. P. Sauvage, *J. Chem. Soc. D* **1971**, 440-&.

64 J. M. Lehn, J. P. Sauvage, B. Dietrich, *J. Am. Chem. Soc.* **1970**, *92*, 2916-2918.

65 B. Dietrich, J. M. Lehn, J. P. Sauvage, *J. Chem. Soc. D* **1970**, 1055-&.

66 B. Dietrich, J. M. Lehn, J. P. Sauvage, *Tetrahedron Lett.* **1969**, 2889-2892.

67 B. Dietrich, J. M. Lehn, J. P. Sauvage, *Tetrahedron Lett.* **1969**, 2885-2888.

68 A. Werner, *Z. Anorg. Allg. Chem.* **1893**, *3*, 267.

69 E. Fischer, *Ber. Dtsch. Chem. Ges.* **1894**, *27*, 2985-2993.

70 E. P. Kyba, R. C. Helgeson, K. Madan, G. W. Gokel, T. L. Tarnowski, S. S. Moore, D. J. Cram, *J. Am. Chem. Soc.* **1977**, *99*, 2564-2571.

71 D. D. MacNicol, J. J. McKendrick, D. R. Wilson, *Chem. Soc. Rev.* **1978**, *7*, 65-87.

72 D. J. Cram, *Angew. Chem. Int. Ed.* **1986**, *25*, 1039-1134.

73 E. Weber, *Top Curr. Chem.* **1987**, *140*, 1-&.

74 G. T. Kokotailo, S. L. Lawton, D. H. Olson, D. H. Olson, W. M. Meier, *Nature* **1978**, *272*, 437-438.

75 G. Alberti, U. Constantino, in *Comprehensive Supramolecular Chemistry, Vol. 7* (Eds.: J. L. Atwood, J. E. D. Davies, D. D. MacNicol, F. Vögtle), Pergamon, Oxford, **1996**, pp. 1-23.

76 B. A. Buffett, *Annu. Rev. Earth Planet. Sci.* **2000**, *28*, 477-507.

77 J. W. Steed, in *Encyclopedia of Supramolecular Chemistry, Vol. 2*, 1 ed. (Eds.: J. L. Atwood, J. W. Steed), Marcel Dekker, Inc., New York, **2004**, pp. 1401-1411.

78 F. Toda, K. Agaki, *Tetrahedron Lett.* **1968**, *9*, 3695-3698.

79 H. Hart, L.-T. W. Lin, D. L. Ward, *J. Am. Chem. Soc.* **1984**, *106*, 4043-4045.

80 W. Baker, A. J. Floyd, J. F. W. McOmie, G. Pope, A. S. Weaving, J. H. Wild, *J. Chem. Soc.* **1956**, 2010-2017.

81 R. Bishop, in *Comprehensive Supramolecular Chemistry, Vol. 6*, 1 ed. (Eds.: J. L. Atwood, J. E. D. Davies, D. D. MacNicol, F. Vögtle), Pergamon, Oxford, **1996**, pp. 85-116.

82 K. D. M. Harris, J. M. Thomas, *J. Chem. Soc., Faraday Trans.* **1990**, *86*, 2985-2996.

83 K. D. M. Harris, J. M. Thomas, *J. Chem. Soc., Faraday Trans.* **1990**, *86*, 1095-1101.

84 F. Diederich, M. Gomez-Lopez, *Chem. Soc. Rev.* **1999**, *28*, 263-277.

85 J. S. Bradshaw, R. M. Izatt, A. V. Bordunov, C. Y. Zhu, J. K. Hathaway, in *Comprehensive Supramolecular Chemistry, Vol. 1*, 1 ed. (Eds.: J. L. Atwood, J. E. D. Davies, D. D. MacNicol, F. Vögtle), Pergamon, Oxford, **1996**, pp. 35-95.

86 E. Maverick, D. J. Cram, in *Comprehensive Supramolecular Chemistry, Vol. 1*, 1 ed. (Eds.: J. L. Atwood, J. E. D. Davies, D. D. MacNicol, F. Vögtle), Pergamon, Oxford, **1996**, pp. 213-243.

87 B. Dietrich, in *Comprehensive Supramolecular Chemistry, Vol. 1*, 1 ed. (Eds.: J. L. Atwood, J. E. D. Davies, D. D. MacNicol, F. Vögtle), Pergamon, Oxford, **1996**, pp. 153-211.

88 J. Szejtli, in *Comprehensive Supramolecular Chemistry, Vol. 3*, 1 ed. (Eds.: J. L. Atwood, J. E. D. Davies, D. D. MacNicol, F. Vögtle), Pergamon, Oxford, **1996**, pp. 1-3.

89 F. Vögtle, C. Seel, P.-M. Windsceif, in *Comprehensive Supramolecular Chemistry, Vol. 2*, 1 ed. (Eds.: J. L. Atwood, J. E. D. Davies, D. D. MacNicol, F. Vögtle), Pergamon, Oxford, **1996**, pp. 211-265.

90 A. Collet, in *Comprehensive Supramolecular Chemistry, Vol. 2*, 1 ed. (Eds.: J. L. Atwood, J. E. D. Davies, D. D. MacNicol, F. Vögtle), Pergamon, Oxford, **1996**, pp. 325-365.

91 E. Maverick, D. J. Cram, in *Comprehensive Supramolecular Chemistry, Vol. 2*, 1 ed. (Eds.: J. L. Atwood, J. E. D. Davies, D. D. MacNicol, F. Vögtle), Pergamon, Oxford, **1996**, pp. 367-418.

92 C. J. Pedersen, *J. Am. Chem. Soc.* **1967**, *89*, 7017-7036.

93 C. D. Gutsche, in *Monographs in Supramolecular Chemistry, Vol. 1* (Ed.: J. F. Stoddart), Royal Society of Chemistry, Cambridge, **1989**.

94 L. R. Nassimbeni, *Acc. Chem. Res.* **2003**, *36*, 631-637.

95 P. J. Nichols, C. L. Raston, J. W. Steed, *Chem. Commun.* **2001**, 1062-1063.

96 M. E. Brown, *Introduction to Thermal Analysis*, Kluwer Academic Publishers, Dordrecht, **2001**.

97 M. P. Suh, Y. E. Cheon, *Aust. J. Chem.* **2006**, *59*, 605-612.

98 L. Dobrzanska, G. O. Lloyd, C. Esterhuysen, L. J. Barbour, *Angew. Chem. Int. Ed.* **2006**, *45*, 5856-5859.

99 L. J. Barbour, *Aust. J. Chem.* **2006**, *59*, 595-596.

100 J. L. Atwood, J. E. D. Davies, D. D. MacNicol, F. Vögtle, Academic Press:Oxford University Press, Oxford, **1991**.

101 J. W. McBain, *The Sorption of Gases by Solids*, Routledge, London, **1932**.

102 B. H. Davis, K. S. W. Sing, in *Handbook of Porous Solids, Vol. 1* (Eds.: F. Schüth, K. S. W. Sing, J. Weitkamp), Wiley, Weinheim, **2002**, pp. 3-23.

103 E. F. Vansant, in *Comprehensive Supramolecular Chemistry, Vol. 7* (Eds.: J. L. Atwood, J. E. D. Davies, D. D. MacNicol, F. Vögtle), Pergamon, Oxford, **1996**, pp. 485-505.

104 L. Schlapbach, A. Zuttel, *Nature* **2001**, *414*, 353-358.

105 V. C. Menon, S. Komarneni, *Journal of Porous Materials* **1998**, *5*, 43-58.

106 R. Coontz, B. Hanson, *Science* **2004**, *305*, 957-957.

107 K. S. W. Sing, D. H. Everett, R. A. W. Haul, L. Moscou, R. A. Pierotti, J. Rouquerol, T. Siemieniewska, *Pure Appl. Chem.* **1985**, *57*, 603-619.

108 J. Rouquerol, D. Avnir, C. W. Fairbridge, D. H. Everett, J. H. Haynes, N. Pernicone, J. D. F. Ramsay, K. S. W. Sing, K. K. Unger, *Pure Appl. Chem.* **1994**, *66*, 1739-1758.

109 A. Nangia, in *Encyclopedia of Supramolecular Chemistry, Vol. 2*, 1 ed. (Eds.: J. L. Atwood, J. W. Steed), Marcel Dekker, Inc., Amsterdam, **2004**, pp. 967-972.

110 H. Lao, C. Detellier, in *Comprehensive Supramolecular Chemistry, Vol. 8* (Eds.: J. L. Atwood, J. E. D. Davies, D. D. MacNicol, F. Vögtle), Pergamon, Oxford, **1996**, pp. 277-306.

111 S. Brunauer, L. S. Deming, W. E. Deming, E. Teller, *J. Am. Chem. Soc.* **1940**, *62*, 1723-1732.

112 W. Zhou, H. Wu, M. R. Hartman, T. Yildirim, *J. Phys. Chem. C* **2007**, *111*, 16131-16137.

113 F. M. Nelsen, F. T. Eggertsen, *Anal. Chem.* **1958**, *30*, 1387-1390.

114 L. Bragg, G. F. Claringbull, in *Crystal Structure of Minerals, Vol. 4*, Cornell University Press, Ithaca, **1965**.

115 S. Kitagawa, R. Kitaura, S. Noro, *Angew. Chem. Int. Ed.* **2004**, *43*, 2334-2375.

116 D. W. Breck, *Zeolite Molecular Sieves*, John Wiley & Sons, Inc., New York, **1974**.

117 H. v. Bekkum, E. M. Flanigen, J. C. Jansen, *Introduction to Zeolite Science and Practice*, Elsevier, Amsterdam, **1991**.

118 M. O. Corp., *Neth. Pat.*, *7, 014,807*, **1971**.

119 D. H. Everett, F. S. Stone, in *The Structure and Properties of Porous Materials*, Butterworths Scientific Publications, London, **1958**.

120 J. L. Atwood, L. J. Barbour, A. Jerga, *Science* **2002**, *296*, 2367-2369.

121 L. J. Barbour, *Chem. Commun.* **2006**, 1163-1168.

122 C. J. Kepert, *Chem. Commun.* **2006**, 695-700.

123 J. C. Bailar, Jr., *Preparative Inorg. Reactions* **1964**, *1*, 1-27.

124 R. M. Barrer, *Molecular Sieves*, American Chemical Society, Washington, **1974**.

125 R. E. Wilde, S. N. Ghosh, B. J. Marshall, *Inorg. Chem.* **1970**, *9*, 2512-2516.

126 H. J. Buser, D. Schwarzenbach, W. Petter, A. Ludi, *Inorg. Chem.* **1977**, *16*, 2704-2710.

127 K. R. Dunbar, R. A. Heintz, *Prog. Inorg. Chem* **1997**, *45*, 283-391.

128 B. F. Hoskins, R. Robson, *J. Am. Chem. Soc.* **1989**, *111*, 5962-5964.

129 B. F. Hoskins, R. Robson, *J. Am. Chem. Soc.* **1990**, *112*, 1546-1554.

130 M. Eddaoudi, J. Kim, N. Rosi, D. Vodak, J. Wachter, M. O'Keefe, O. M. Yaghi, *Science* **2002**, *295*, 469-472.

131 O. M. Yaghi, M. O'Keeffe, N. W. Ockwig, H. K. Chae, M. Eddaoudi, J. Kim, *Nature* **2003**, *423*, 705-714.

132 N. W. Ockwig, O. Delgado-Friedrichs, M. O'Keeffe, O. M. Yaghi, *Acc. Chem. Res.* **2005**, *38*, 176-182.

133 A. K. Cheetham, C. N. R. Rao, R. K. Feller, *Chem. Commun.* **2006**, 4780-4795.

134 H. Li, M. Eddaoudi, M. O'Keeffe, O. M. Yaghi, *Nature* **1999**, *402*, 276-279.

135 E. J. Cussen, J. B. Claridge, M. J. Rosseinsky, C. J. Kepert, *J. Am. Chem. Soc.* **2002**, *124*, 9574-9581.

136 O. Saied, T. Maris, J. D. Wuest, *J. Am. Chem. Soc.* **2003**, *125*, 14956-14957.

137 K. Yamada, H. Tanaka, S. Yagishita, K. Adachi, T. Uemura, S. Kitagawa, S. Kawata, *Inorg. Chem.* **2006**, *45*, 4322-4324.

138 S. Takamizawa, K. Kojima, T. Akatsuka, *Inorg. Chem.* **2006**, *45*, 4580-4582.

139 X. Q. Wang, L. M. Liu, A. J. Jacobson, *Angew. Chem. Int. Ed.* **2006**, *45*, 6499-6503.

140 A. T. Ung, D. Gizachew, R. Bishop, M. L. Scudder, I. G. Dance, D. C. Craig, *J. Am. Chem. Soc.* **1995**, *117*, 8745-8756.

141 T. Dewa, K. Endo, Y. Aoyama, *J. Am. Chem. Soc.* **1998**, *120*, 8933-8940.

142 K. T. Holman, A. M. Pivovar, J. A. Swift, M. D. Ward, *Acc. Chem. Res.* **2001**, *34*, 107-118.

143 P. K. Thallapally, B. P. McGrail, S. J. Dalgarno, H. T. Schaef, J. Tian, J. L. Atwood, *Nat. Mater.* **2008**, *7*, 146-150.

144 C. Serre, F. Millange, C. Thouvenot, M. Nogues, G. Marsolier, D. Louer, G. Ferey, *J. Am. Chem. Soc.* **2002**, *124*, 13519-13526.

145 P. L. Llewellyn, S. Bourrelly, C. Serre, Y. Filinchuk, G. Ferey, *Angew. Chem. Int. Ed.* **2006**, *45*, 7751-7754.

146 S. Kitagawa, K. Uemura, *Chem. Soc. Rev.* **2005**, *34*, 109-119.

147 L. Dobrzanska, G. O. Lloyd, H. G. Raubenheimer, L. J. Barbour, *J. Am. Chem. Soc.* **2006**, *128*, 698-699.

148 J. L. Atwood, L. J. Barbour, A. Jerga, B. L. Schottel, *Science* **2002**, *298*, 1000-1002.

149 J. W. Steed, *Science* **2002**, *298*, 976-977.

150 S. Takamizawa, M. A. Kohbara, *Dalton Trans.* **2007**, 3640-3645.

151 J. L. Atwood, L. J. Barbour, A. Jerga, *Angew. Chem. Int. Ed.* **2004**, *43*, 2948-2950.

152 J. L. Atwood, L. J. Barbour, P. K. Thallapally, T. B. Wirsig, *Chem. Commun.* **2005**, 51-53.

153 P. K. Thallapally, G. O. Lloyd, T. B. Wirsig, M. W. Bredenkamp, J. L. Atwood, L. J. Barbour, *Chem. Commun.* **2005**, 5772-5774.

154 P. K. Thallapally, B. P. McGrail, J. L. Atwood, *Chem. Commun.* **2007**, 1521-1523.

CHAPTER 2

EXPERIMENTAL TECHNIQUES

The work presented in this thesis has involved the use of several common instrumental techniques and much routine methodology. Since these are already well-documented, they are only briefly described in this chapter. Other apparatus and procedures developed specifically as part of this work are discussed in greater detail. Where appropriate, additional instrumental and synthetic protocols will be elaborated on in the chapters that follow.

2.1 SINGLE-CRYSTAL X-RAY DIFFRACTION (SCD)

Intensity data were collected on a Bruker SMART Apex CCD diffractometer[1] using graphite monochromated Mo-K_α radiation (λ = 0.71073 Å). The temperature of the crystals was controlled using an Oxford Cryostream Cooler. Data reduction was carried out by means of a standard procedure using the Bruker software package SAINT.[2] Where necessary, systematic errors in the intensity data were corrected for using SADABS.[3,4] The structures were solved by direct methods or a combination of Patterson and partial structure expansion using SHELXS-97.[5] In most cases, all non-hydrogen atoms were located using either of these methods. All ordered non-hydrogen atoms were refined anisotropically by means of full-matrix least squares calculations on F^2 using SHELXL-97[5] within the X-Seed[6] environment. Where appropriate, the hydrogen atoms were placed in calculated positions using riding models and assigned isotropic thermal parameters 1.2 times those of their parent atoms for CH_2, aromatic C and O-H groups, or 1.5 times those of their parent atoms for CH_3 groups. In special cases, hydrogen atoms were located in difference electron density maps and their isotropic thermal parameters were refined freely.

The supplementary material for all crystal structures elucidated as part of this study can be found on the attached CD, including the Crystallographic Information Files (CIF) along with the final SHELX '.res' and '.hkl' files.

2.2 X-RAY POWDER DIFFRACTION (XRPD)

X-ray powder diffraction experiments were carried out on a Bruker D8 Advance instrument using Cu-K_α radiation (λ = 1.5418 Å) and a point detector. Intensity data were collected using multiple θ-θ scans. Sample preparation included grinding of the material with a mortar and pestle and the sample was rotated (at 15 rpm) during data collection to minimise effects due to preferred orientation. Care was also taken when packing powders into sample holders to minimise peak displacement errors due to sample height inconsistencies.

Where necessary, XRPD patterns were calculated from single-crystal X-ray structures using Lazy Pulverix[7] within the X-Seed[6] graphical interface.

All figures showing intensity data for experimental and calculated patterns were plotted using Microsoft Excel.

2.3 THERMOGRAVIMETRIC ANALYSIS (TGA)

Thermogravimetric analysis was carried out using a TA Instruments Q500 thermogravimetric analyser. The balance and sample were purged with dry N_2 gas flowing at rates of 50 and 70 $cm^3.min^{-1}$. Samples were heated at a rate of either 5 or 10 $^oC.min^{-1}$. All post-experimental analyses were carried out using the TA Instruments Universal Analysis program and figures were prepared using Microsoft Excel.

2.4 DIFFERENTIAL SCANNING CALORIMETRY (DSC)

Differential scanning calorimetry was performed using a TA Instruments Q100 differential scanning calorimeter. All samples were prepared by crimping the sample pan and lid tightly after two pin holes were made in the lid. A reference pan was prepared in exactly the same manner for each sample. Samples of 2-10 mg were heated at a rate of 2.5 or 5 $^oC.min^{-1}$ from ambient temperature to 160 or 180 ^oC (in the case of organic compounds) or from ambient temperature to *ca* 500 ^oC (for coordination compounds). Samples were purged at a flow rate of 50 $cm^3.min^{-1}$. All

post-experimental analyses were carried out using the TA Instruments Universal Analysis program and figures were prepared using Microsoft Excel.

2.5 GRAVIMETRIC GAS SORPTION

Gravimetric sorption isotherms were measured using an Intelligent Gravimetric Analyser (IGA-002) (Figure 2.1) supplied by Hiden Analytical (Ltd), Warrington, UK.[8] Only ultra-high purity gasses were used. The instrument facilitates precise measurement of mass change and control of pressure and temperature, and is equipped with an enhanced pressure rating that allows measurements up to 20 bar. The pressure is monitored using a pressure transducer with a range of 0-20 bar and buoyancy effects are corrected for automatically by the control software. An accurate estimate of the sample density is required for the buoyancy correction – this can be determined either from the single-crystal structure or, in the absence of a structure, by means of a buoyancy scan under helium pressure. Temperature control is maintained to an accuracy of +/- 0.05 °C using a Grant refrigerated recirculating bath.

Data collection on the IGA is controlled by Real-Time Processing computer software,[9-15] which continually checks for pressure/weight equilibrium using least-squares regression to extrapolate a value of the asymptote. In the present study, a Linear Driving Force (LDF) relaxation model was used, with each equilibrium point recorded only once a 99% fit with the model was achieved.

Each sample was subjected to an outgas sequence to ensure guest- and vapour-free material before sorption runs commenced. The same outgas sequence was also followed between consecutive runs of the same sample when either the temperature or gas were changed. After collection of the sorption isotherms, the IGA system software offers a range of output formats in which to save the data. For the purposes of this study, values of mmol gas per gram host as a function of equilibrium pressure were selected. From these data, occupancy can be calculated using the expected host:guest ratio (as inferred from single-crystal structures) and the molar mass of the host molecules.

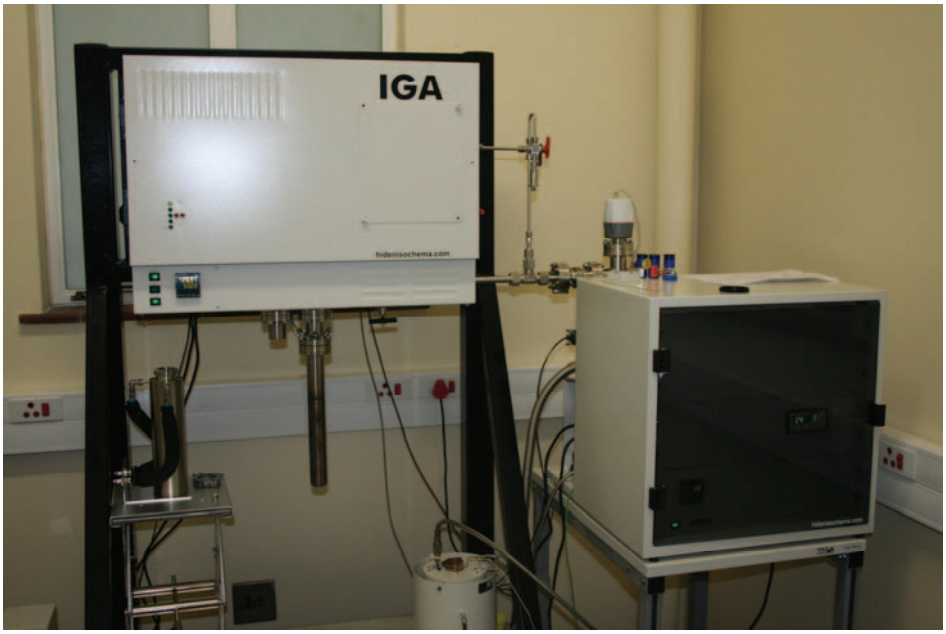

Figure 2.1 Photographs of the Hiden Intelligent Gravimetric Analyser (IGA-002).

2.6 VOLUMETRIC GAS SORPTION

The HIDEN gravimetric sorption analyser cannot be used to study the sorption of acetylene because the balance mechanism contains a winding of copper wire – exposure of pure copper metal to acetylene gas poses an explosion hazard. A second drawback of the gravimetric sorption analyser is its inability to perform measurements beyond 20 bar. Instead, a locally-constructed volumetric sorption system (Figure 2.2) was used for acetylene gas and higher pressure work. The design and operation of this system has been reported in the literature.[16]

a

b

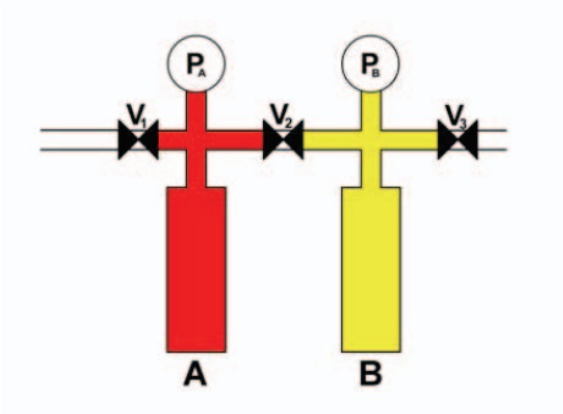

Figure 2.2 **(a)** A photograph of the locally-constructed volumetric gas sorption device. **(b)** A schematic of the volumetric device – indicating reservoirs **A** and **B**, valves 1-3 ($\mathbf{V_1}$-$\mathbf{V_3}$) and electronic pressure transmitters $\mathbf{P_A}$ and $\mathbf{P_B}$.

In a typical experiment, electronic pressure transmitters accurately record the change in pressure as a function of time while the volume and temperature of the reservoir and sample chambers remain fixed. The system consists of three valves ($\mathbf{V_1}$-$\mathbf{V_3}$), a reservoir chamber on the left (**A**) and a sample chamber on the right (**B**), and electronic pressure sensors ($\mathbf{P_A}$ and $\mathbf{P_B}$) transmitting readings for each of the chambers to a computer. The volumes of the empty chambers V_A and V_B are calibrated as described in Figure 2.3 (steps a-e) using nitrogen gas at low pressures, and an aluminium rod of known volume (the ideal gas law is assumed – Equation 2.1).

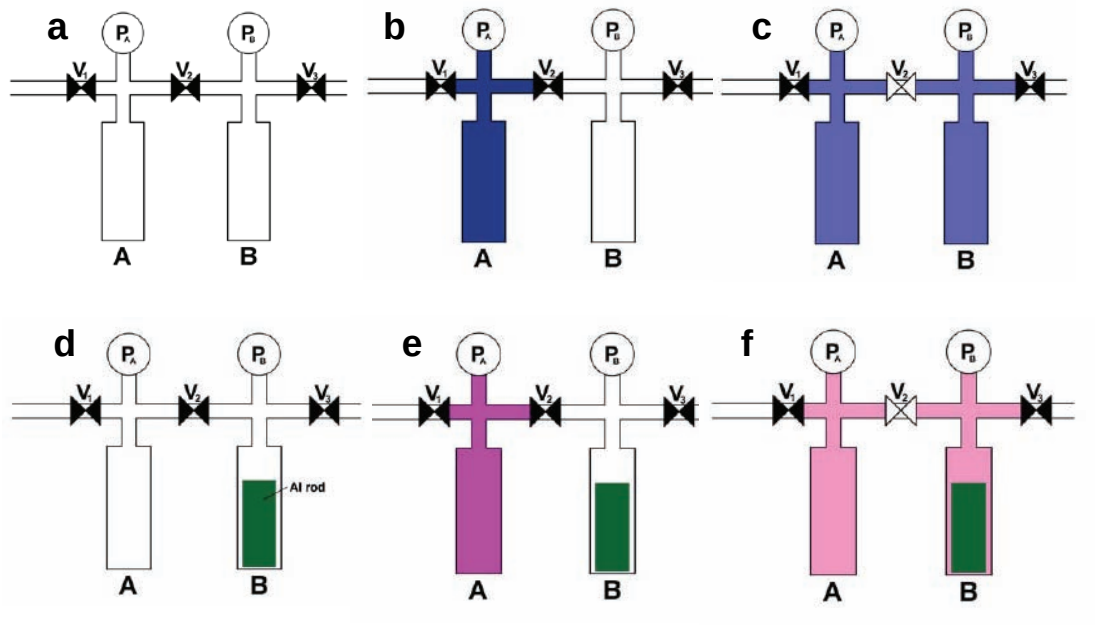

Figure 2.3 Schematic showing how the volumes of the chambers **A** and **B** are calculated. **(a)** The entire system is evacuated and all three valves are closed. **(b)** N_2 is introduced into Chamber **A** and the pressure reading of $\mathbf{P_A}$ is recorded as P_1. **(c)** $\mathbf{V_2}$ is opened and the N_2 is allowed to equilibrate throughout chambers **A** and **B** and a new value for $\mathbf{P_A}$ (which should be the same as $\mathbf{P_B}$) is recorded as P_2. **(d)** N_2 is released from the system and an aluminium rod of known volume V_X is placed in chamber **B**. The available volume in this chamber is now (V_B - V_X) and the system is once again evacuated and all three valves closed. **(e)** N_2 is introduced into Chamber **A** as in (b) and the pressure reading of $\mathbf{P_A}$ is recorded as P_3. **(f)** $\mathbf{V_2}$ is opened as in (c) and the pressure of $\mathbf{P_A} = \mathbf{P_B}$ recorded as P_4.

$$pV = nRT \qquad (2.1)$$

From steps a-c we have:

$$P_1 V_A = P_2 (V_A + V_B)$$

which rearranges to:

$$\frac{P_1}{P_2} = \frac{(V_A + V_B)}{V_A} = 1 + \frac{V_B}{V_A} \qquad (2.2)$$

After a known volume of aluminium rod (V_X) is introduced we have for steps d-f:

$$P_3 V_A = P_4 (V_A + V_B - V_X)$$

or

$$\frac{P_3}{P_4} = \frac{(V_A + V_B - V_X)}{V_A} = 1 + \frac{V_B}{V_A} - \frac{V_X}{V_A} \qquad (2.3)$$

Using equations 2.2 and 2.3 we can now firstly calculate V_A and consequently, V_B. The free volume of sample chamber **B** is determined by subtracting the volume of the sample (the mass of the sample is known and the density is determined from single-crystal X-ray diffraction) from V_B.

The volumetric sorption apparatus shown in Figure 2.2a is installed in an insulated cabinet which is thermostated using three 60 Watt light bulbs and a circulating fan. The temperature is monitored by computer software and controlled using a simple on-off protocol. All sorption isotherms were determined at a temperature of 22 ºC. The number of moles of gas molecules was calculated by solving the van der Waals Equation of State (equation 2.4) using customised software.

$$\left(P + \frac{n^2 a}{V^2}\right)(V - nb) = nRT \qquad (2.4)$$

Figure 2.4 shows the output for a typical sorption experiment. $P1_{start}$ is the reading of $\mathbf{P_A}$ after the gas is introduced into chamber **A** and allowed to equilibrate. A drop in pressure is seen for the blue curve when $\mathbf{V_2}$ is opened for *ca* 1 second to allow gas into chamber **B**. As soon as gas is introduced into chamber **B**, it is sorbed by the sample and this is evident in the behaviour of the green curve. When the sorption process reaches equilibrium (when P_2 no longer changes with time) the value of $P2_{eq}$ is recorded as the equilibrium pressure. Using the van der Waals equation, V_A, $P1_{start}$ and $P1_{end}$, the number of moles of gas introduced into chamber **B** can be calculated. Using the free volume (V_B) and the equilibrium pressure $P2_{eq}$, the amount of supernatant gas in sample chamber **B** can be determined and, consequently, the total amount of sorbed gas. Occupancy can then be determined at $P2_{eq}$ using the molar amount of sample and the host:guest ratio. After a series of such experiments (*i.e.* recharging the reservoir and allowing gas into the sample chamber) in which the equilibrium pressure is increased systematically, a curve of occupancy against equilibrium loading pressure can be plotted.

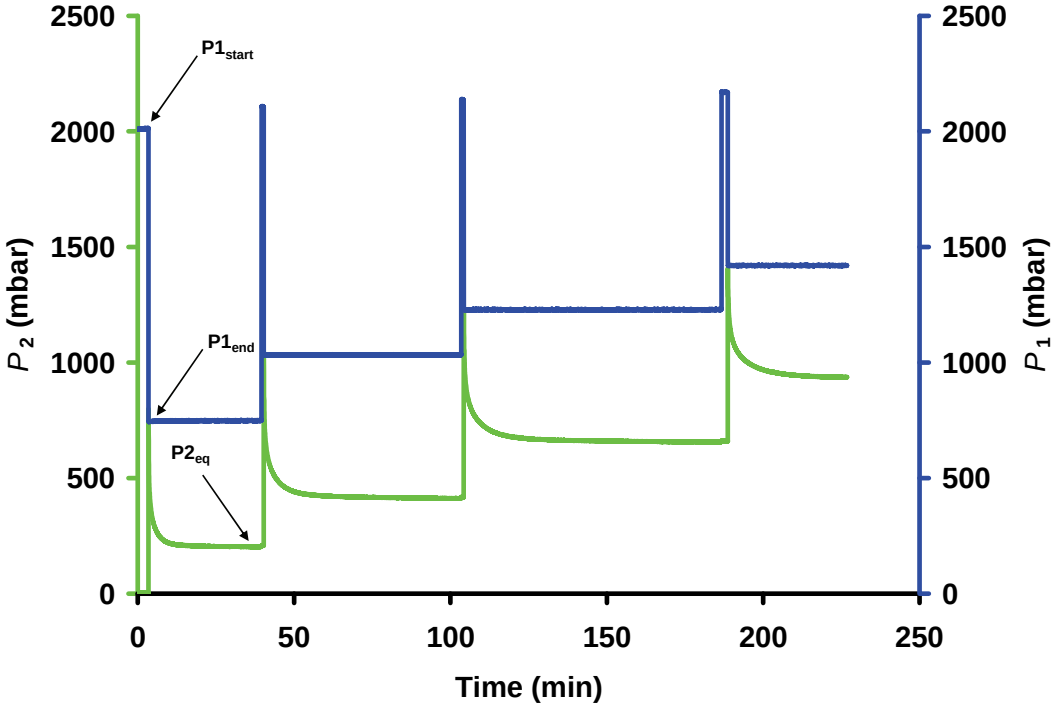

Figure 2.4 Output from a typical gas sorption experiment in which four consecutive sorption runs are recorded with increasing equilibrium pressure and no evacuation between successive steps. P_1 is the pressure in sample chamber **A** and P_2 the pressure in sample chamber **B**.

2.7 GAS CELL FOR COLLECTION OF SINGLE-CRYSTAL DATA UNDER CONTROLLED ATMOSPHERES

Crystal structures from intensity data collection with the crystal under gas pressure were initially determined using a device similar to that displayed in Figure 2.5. Typically, a suitable crystal is selected and glued to the end of a glass microfiber which, in turn, is inserted and glued into a 3 mm glass capillary that had been pre-sealed at the narrow end using a small flame. The capillary is fixed to the end of a stainless steel tube (0.25 inch outer diameter) with copious amounts of epoxy resin in order to render the glass-to-metal seal leak-proof (Figure 2.5a). The steel tube is fixed into a Swagelok brass union cross to which are also attached an analogue pressure gauge (to monitor pressure within the apparatus) and a valve to allow gas uptake/release (Figure 2.5b). This device is fixed by means of a standard *x*-*y* goniometer head to the omega-stage of the diffractometer and the crystal is centred in the X-ray beam (Figure 2.5c). Single-crystal diffraction data are then collected using

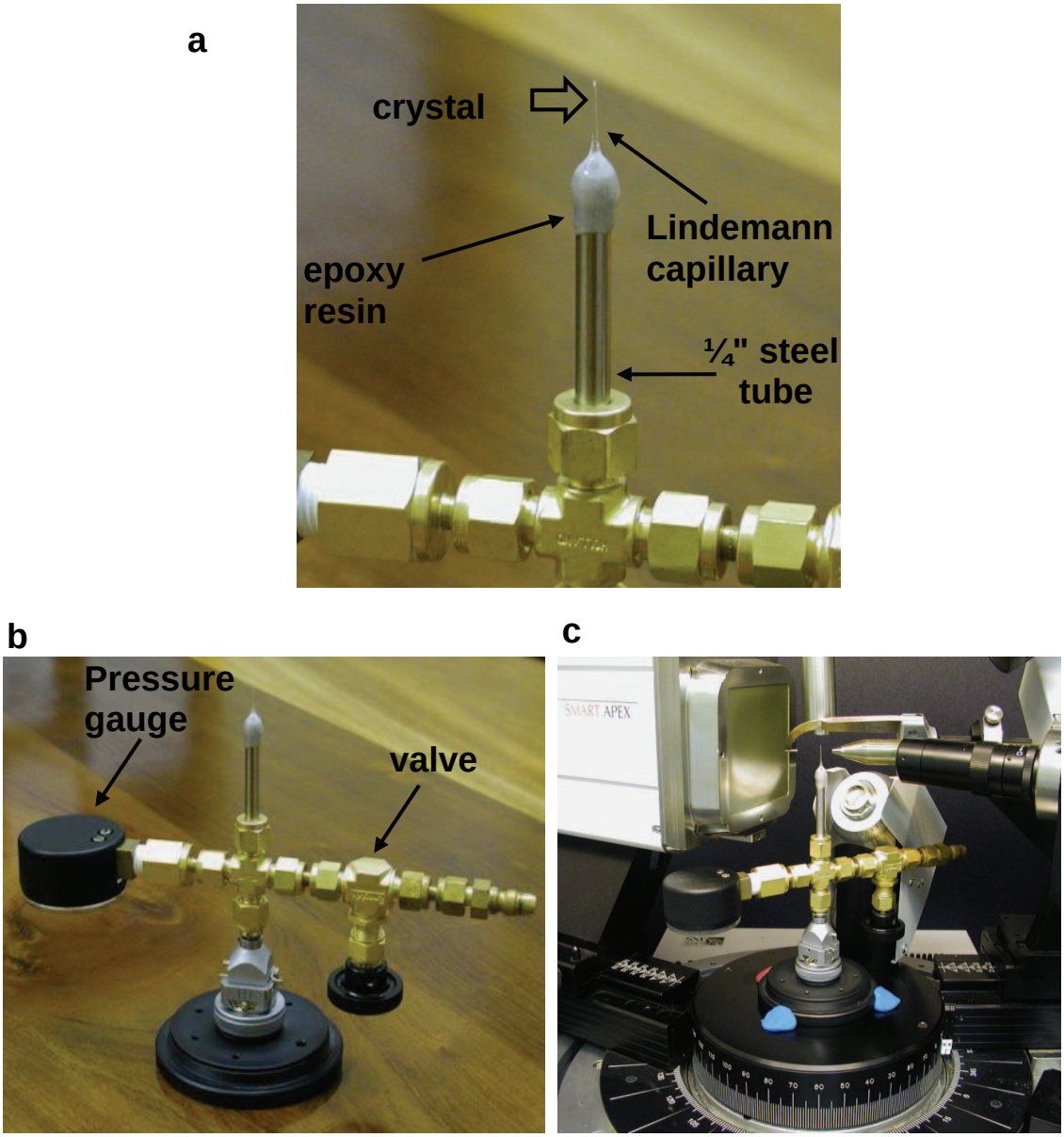

Figure 2.5 Apparatus for determining crystal structures under controlled gaseous atmosphere. **(a)** A crystal is glued onto a glass microfiber which is then glued into a glass capillary. The capillary is fixed to the tip of a stainless steel tube using epoxy resin. **(b)** The entire leak-proof device including a valve for gas uptake/release and a pressure gauge. **(c)** The device is fixed onto the omega-stage of the diffractometer and reflection data are collected by rotation around this axis.

an unconventional data collection strategy – *i.e.* an overall 180° rotation about the omega axis in steps of -0.3°, with the detector positioned at 2θ = -28°.

Owing to its size, the prototypical gas cell described above is too unwieldy to make use of the diffractometer's phi axis. This limitation necessitates a data collection strategy that is insufficient even for collecting a full quadrant of data, let alone enough

redundant data for empirical corrections of systematic errors. A miniaturised pressure cell was therefore developed in order to implement a routine data collection strategy.

The miniature gas cell consists of three parts: (i) a stainless steel fitting to which a glass capillary containing the crystal is attached, (ii) a brass cell equipped with a port for the steel fitting, a valve stem and a gas inlet port, and (iii) a removable gas inlet arm which attaches to the brass cell during gas loading (Figure 2.6a and b).

a

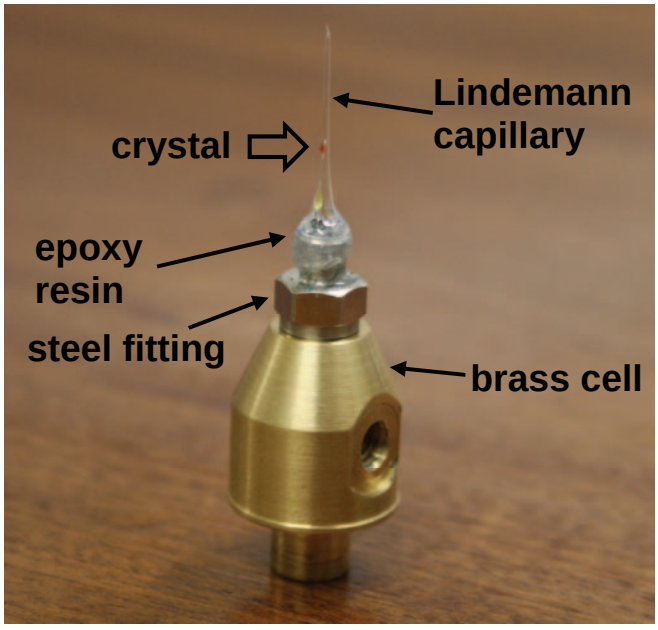

b

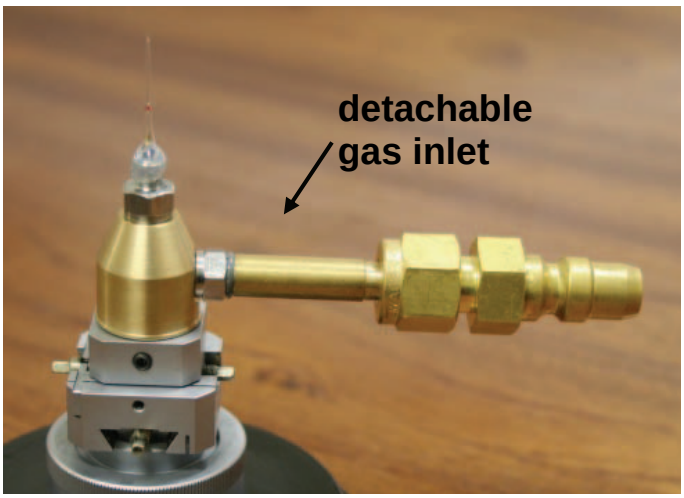

c

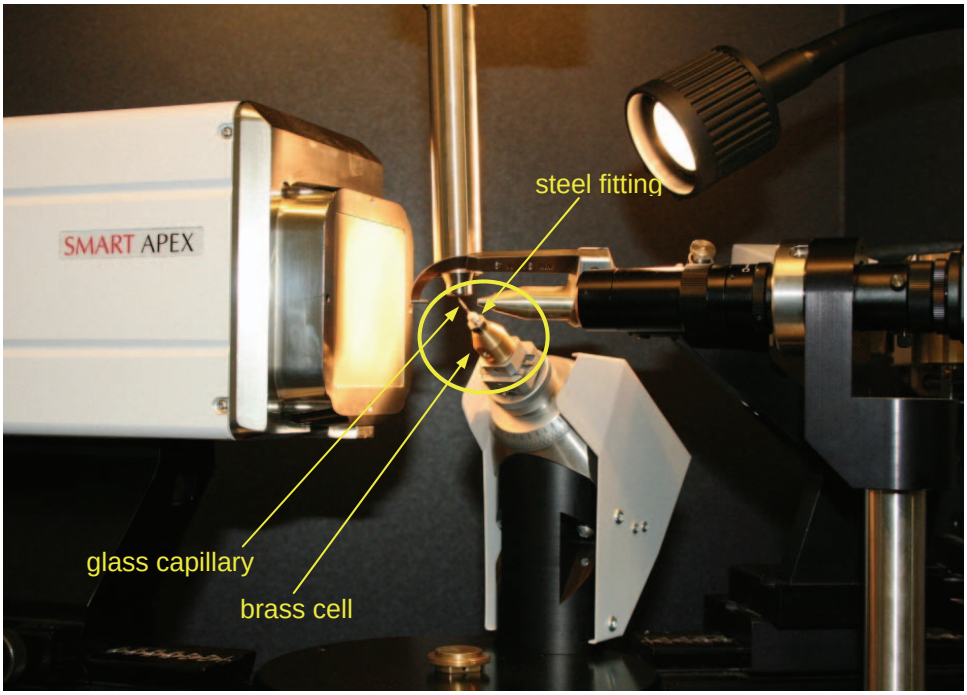

Figure 2.6 **(a)** Miniature gas cell. **(b)** Gas cell with detachable gas inlet. **(c)** The gas cell attached to the goniometer of a Bruker-Nonius SMART Apex diffractometer.

The first part of the crystal preparation procedure is similar to that for the original gas cell. A suitable crystal is attached to the end of a thin (< 0.1 mm) glass rod by means of epoxy resin. The glass rod is then inserted into a glass capillary (300 μm outer diameter, 10 μm wall thickness) and fixed to the interior of the capillary, again using epoxy resin. The capillary is flame-sealed at one end and the open end is fixed to an opening at one end of the steel fitting (using epoxy resin). In order to ensure a gas-tight seal between the capillary and the steel fitting, the epoxy resin is allowed to cure overnight. The steel fitting is screwed onto the brass cell and the seal between the fitting and the cell is secured by means of a rubber o-ring. The detachable gas inlet arm is attached to the side of the brass cell and to the regulator of a gas cylinder. The gas cell is charged with gas by adjusting the regulator to the required pressure, after which the cell is sealed by means of the valve stem. After detaching the gas inlet arm, the gas cell can be mounted on a conventional X-ray diffractometer by means of a standard goniometer head (Figure 2.6c).

Owing to the compact design of the cell, it is not possible to measure the pressure *in situ* once the cell has been sealed using the valve stem – after sealing, the pressure is assumed to be that set by the regulator of the gas cylinder and it is also assumed that

no leaks occur. The integrity of the individual parts against leaks can be tested separately and the apparatus has been verified as leak-proof even at pressures up to 80 bar.

2.8 ELECTRON DENSITY STUDIES

The occupancy from the single-crystal structures was determined using PLATON[17,18]/SQUEEZE[19] which calculates the electron contribution of the guest molecules. The final occupancy can then be determined from the electron-count calculated by SQUEEZE – by comparison to the known number of electrons in the guest molecule(s). According to the SQUEEZE manual: "The SQUEEZE procedure takes care of the contribution of a (heavily) disordered solvent to the calculated structure factors by back-Fourier transformation of the continuous density found in a masked region of the difference map. The masked region is defined as the solvent accessible region left by the ordered part of the structure." The calculation yields, among other values, the void volume and the number of electrons in the void. Under normal circumstances one would expect this electron count to match that expected for the presumed solvent. It is noted however, that the method relies on high resolution data and that if the dataset does not fulfil this requirement, the accuracy of the results may be questionable. SQUEEZE calculations were performed for structures with the included CCl_4, CH_3OH, C_2H_2, CO_2, COS and CS_2 deleted as appropriate. In no instance was SQUEEZE used to modify the '.hkl' file to obtain F_o^2 data without solvent contributions. Therefore the SQUEEZE '.sqf' output file in CIF format was not appended to the CIF file for each structure, but can be viewed separately as part of the supplementary data.

2.9 GRAPHICAL REPRESENTATION AND CALCULATIONS OF VOLUMES AND GUEST-ACCESSIBLE SURFACES

The program[20] POV-Ray™ (which is also accessible *via* X-Seed) was used to produce high quality molecular graphics. Where necessary, unit cell and atomic labels were embedded into the graphics using POV-Label.

Guest-accessible surfaces were calculated using the program MSROLL[21,22] which was developed by Michael L. Connolly and which can also be accessed within the X-Seed[6,23] interface. The program was originally designed to map the solvent-accessible areas of proteins and nucleic acids for graphical display. Lee and Richards[24] defined the solvent-accessible area as the surface area created by tracing the centre of a sphere with a known radius as it is rolled around the surface of interest. The method only provides a numerical value for this area and is subsequently not applicable for visualisation of the void for which it also does not calculate the volume. In order to be able to visualise the solvent accessible volume, an alternative approach was suggested by Richards[25] where a smoothing function would be utilised to negate the areas between the atoms that are inaccessible to the probe sphere as it traces its route along the surface of the void. The smoothing function replaces the inaccessible fissures with "concave and saddle shaped surfaces", thereby excluding regions that are unable to produce a van der Waals interaction with the solvent molecule. The advantage is that only the total surface area that is accessible to the probe sphere is considered and extension into visualising the solvent-accessible surface is possible. Connolly used this definition and, along with the existing dot surface algorithm, developed a new analytical surface algorithm in order to generate high-resolution colour raster images and to calculate more precise molecular areas and volumes.

In the present study, for the purposes of calculating volumes and visualising cavities in single-crystal structures, the guests (usually solvent or gas molecules) are first removed from the atom list. MSROLL is then called after setting an appropriate probe radius. When cavities can be mapped in a structure a '.cav' file is created which can be imported into X-Seed for visualisation as part of the structure using POV-Ray (Figure 2.7a). Images are often rendered with guest molecules reinstated to show the interaction between host atoms and guest molecules, as well as the location of the latter within the guest-accessible voids (Figure 2.7b). As can be seen in the figure, the guest methanol molecules protrude from the mapped grey surface. This means that the van der Waals surfaces of the guest molecules and host framework are overlapping, *i.e.* an intermolecular interaction is inferred, and this phenomenon is therefore often observed for inclusion compounds.

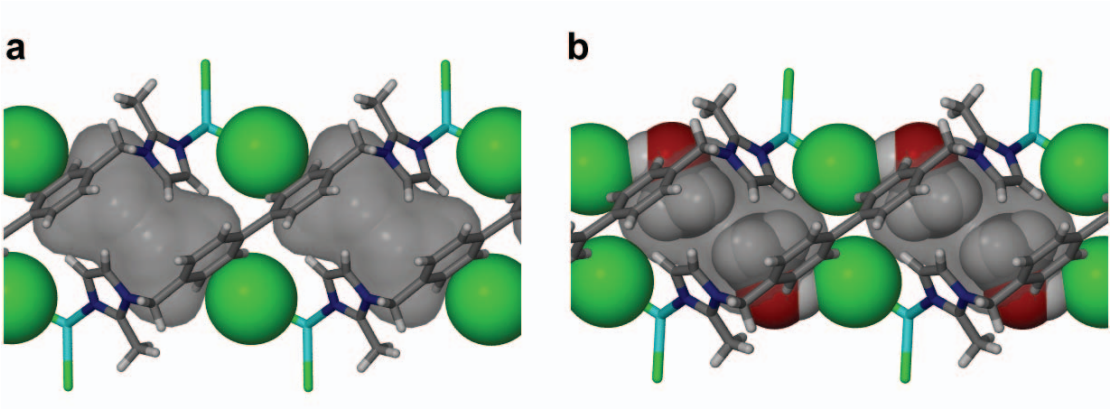

Figure 2.7 **(a)** Two discrete mapped cavities are shown as semi-transparent grey surfaces that are in van der Waals contact with the host framework. **(b)** The guest methanol molecules protrude from the grey surface and are overlapping slightly with the host chloride ions (shown as green spheres).

2.10 VAN DER WAALS RADII

In consulting the literature it becomes clear that there is little consensus on acceptable values for the van der Waals radii of the various atoms. The values specified by Pauling[26] and Bondi[27] are most commonly used in connection with molecular crystals. Bondi and others agree that the value of the van der Waals radius of an atom is affected by the nature of the atoms it is bonded to, as well as the nature of the bonds themselves.[28] To further complicate the situation, it has been noted that many atoms may be non-spherical, with a shortening of the radius along the direction of the bond.[27,28] It is thus clear that many factors influence the van der Waals radius of an atom and these factors most likely vary from one structure to the next. In this study one set of values was selected for van der Waals radii of all the elements used (summarised in Table 2.1).[*] Where appropriate, these values are used in space-filled representations of crystal structures and geometrical calculations (such as cavity volume determinations in MSROLL). It is acknowledged here that treatment of atoms (and their corresponding ions) as spheres of constant radius is not ideal, but also that a superior method that is simple to implement has not yet been proposed.

[*] The van der Waals radii chosen are the default values used in the X-Seed software and were selected from the van der Waals radii values specified by Pauling and Bondi.

Table 2.1 Van der Waals Radii used in the present study.

Atom	Radius (Å)	Atom	Radius (Å)
H	1.20	Br	1.93
C	1.70	I	1.98
N	1.55	Co	0.65
O	1.52	Zn	0.74
S	1.80	Cd	0.95
Cl	1.80		

It should also be stated that cations and anions most likely do not have the same van der Waals radii as their corresponding neutral atoms. A literature survey of van der Waals radii of the halides used in this study reveals that the radii of chlorine and bromine are thought to remain largely unchanged when they are ionised (r = 1.81 Å for Cl^- and r = 1.96 Å for Br^-), while iodine shows a greater increase in size from r = 1.98 Å for iodine to r = 2.20 Å for iodide.[29] Once again the van der Waals radii of ions also depend on numerous factors, and the accepted values are not necessarily accurate indications of the most appropriate radii for a specific structure. In light of this, it has been decided to use the van der Waals radius of the neutral atoms for the halide anions in all cases. Where deemed appropriate, a discussion of the effect of the increased atom/ion size is included in the relevant text.

REFERENCES

1 *SMART Data Collection Software*, Version 5.629, Bruker AXS Inc., Madison, WI, **2003**.

2 *SAINT Data Reduction Software*, Version 6.45, Bruker AXS Inc., Madison, WI, **2003**.

3 *SADABS*, Version 2.05, Bruker AXS Inc., Madison, WI, **2002**.

4 R. H. Blessing, *Acta Crystallogr., Sect. A: Found. Crystallogr.* **1995**, *51*, 33-38.

5 G. M. Sheldrick, *Acta Crystallogr., Sect. A: Found. Crystallogr.* **2008**, *64*, 112-122.

6 L. J. Barbour, *Journal of Supramolecular Chemistry* **2001**, *1*, 189-191.

7 K. Yvon, W. Jeitschko, E. Parthe, *J. Appl. Crystallogr.* **1977**, *10*, 73-74.

8 M. J. Benham, D. K. Ross, *Z. Phys. Chem. (Muenchen, Ger.)* **1989**, *163*, 25-32.

9 A. J. Fletcher, K. M. Thomas, *Langmuir* **1999**, *15*, 6908-6914.

10 A. J. Fletcher, K. M. Thomas, *Langmuir* **2000**, *16*, 6253-6266.

11 N. J. Foley, K. M. Thomas, P. L. Forshaw, D. Stanton, P. R. Norman, *Langmuir* **1997**, *13*, 2083-2089.

12 A. W. Harding, N. J. Foley, P. R. Norman, D. C. Francis, K. M. Thomas, *Langmuir* **1998**, *14*, 3858-3864.

13 I. P. Okoye, M. Benham, K. M. Thomas, *Langmuir* **1997**, *13*, 4054-4059.

14 C. R. Reid, I. P. O'Koye, K. M. Thomas, *Langmuir* **1998**, *14*, 2415-2425.

15 C. R. Reid, K. M. Thomas, *Langmuir* **1999**, *15*, 3206-3218.

16 J. L. Atwood, L. J. Barbour, P. K. Thallapally, T. B. Wirsig, *Chem. Commun.* **2005**, 51-53.

17 *PLATON, A Multipurpose Crystallographic Tool*, Utrecth University, Utrecht, The Netherlands, **2008**.

18 A. L. Spek, *J. Appl. Crystallogr.* **2003**, *36*, 7-13.

19 P. van der Sluis, A. L. Spek, *Acta Crystallogr., Sect. A: Found. Crystallogr.* **1990**, *46*, 194-201.

20 *POV-Ray™ for Windows*, Version 3.6, Persistence of Vision Raytracer Pty. Ltd., Williamstown, Australia, **2004**, *http://www.povray.org*.

21 M. L. Connolly, *Science* **1983**, *221*, 709-713.

22 M. L. Connolly, *J. Mol. Graphics* **1993**, *11*, 139-143.

23 J. L. Atwood, L. J. Barbour, *Cryst. Growth Des.* **2003**, *3*, 3-8.

24 B. Lee, F. M. Richards, *J. Mol. Biol.* **1971**, *55*, 379-400.

25 F. M. Richards, *Annu. Rev. Biomed. Eng.* **1977**, *6*, 151-176.

26 L. Pauling, *The Nature of the Chemical Bond*, Cornell University Press, Ithaca, **1942**.

27 A. Bondi, *J. Phys. Chem.* **1964**, *68*, 441-451.

28 S. C. Nyburg, C. H. Faerman, *Acta Crystallogr., Sect. B: Struct. Sci.* **1985**, *41*, 274-279.

29 R. D. Shannon, *Acta Crystallogr., Sect. A: Found. Crystallogr.* **1976**, *32*, 751-767.

CHAPTER 3

CRYSTAL ENGINEERING OF DIANIN'S COMPOUND

3.1 INTRODUCTION

Dianin's compound (DC, or **1**) was first synthesised by A. P. Dianin in 1914 from phenol and mesityl oxide (Scheme 3.1).[1] Since then it has become one of the most well-known and versatile organic hosts in the field of inclusion chemistry. In 1955 the molecular structure (incorrectly proposed by Dianin as 2-*p*-hydroxyphenyl-2,2,4-trimethylchroman) was re-assessed by Baker and McOmie and unambiguously determined as 4-*p*-hydroxyphenyl-2,2,4-trimethylchroman.[2] The crystal structure of DC was correctly proposed (although not determined) by Powell and Wetters[3] but, prior to this[1,2] and without crystallographic data,[4] studies had already reported some inclusion behaviour of DC.

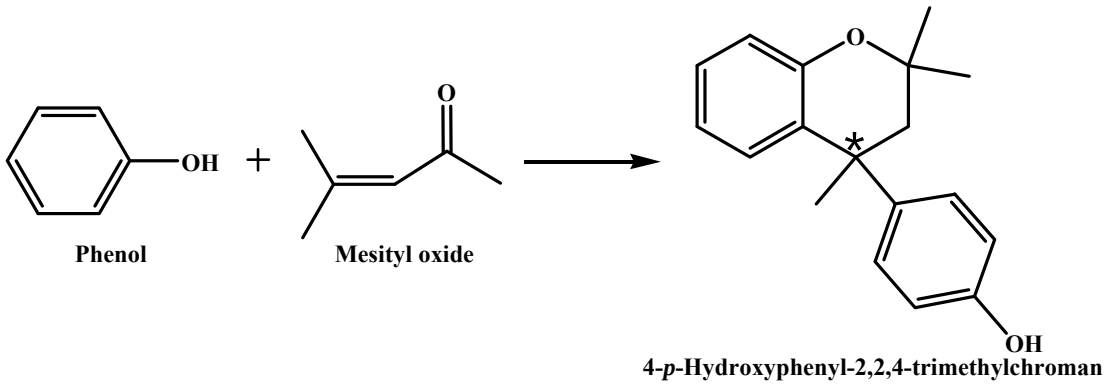

Scheme 3.1 Dianin's compound (**1**) is synthesised by the condensation of phenol and mesityloxide (the asterisk indicates the chiral centre of the molecule).

The first single-crystal structure of **1** as an organic clathrate, crystallising in the high symmetry space group $R\bar{3}$, was published in 1970 by Flippen *et al*.,[5] marking the start of many subsequent crystallographic studies of the inclusion behaviour of DC. In the absence[6] or presence of a wide selection of guests, the Dianin's host system has always produced the typical hexagonal hydrogen bonded arrangement (Figure 3.1), which is well-established as the major structure-directing feature of this system. Racemic **1** forms clathrates where six molecules of the host are hydrogen bonded to

one another by means of their hydroxy groups to form a hexagonal ring. The ring consists of three molecules of identical chirality pointing upwards (R_1 in Figure 3.1) and three molecules of the opposing chirality pointing downwards (R_2 in Figure 3.1).

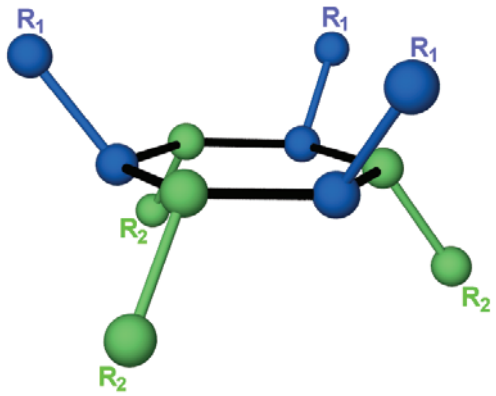

Figure 3.1 The racemate of DC typically crystallises with six molecules positioned about a site of $\bar{3}$ symmetry, forming a hexameric O–H···O hydrogen bonded cyclic arrangement with three molecules situated above the resulting hydrogen bonded ring plane and their three enantiomers positioned below the plane.

These hexameric units stack over one another such that the enantiomers interdigitate to form hourglass-shaped cavities (*ca* 220 Å^3, r_{probe} = 1.6 Å), with a six-membered ring forming the floor of each cavity, and another forming the ceiling (Figure 3.2). These components pack along the hexagonal *c*-axis (perpendicular to the hydrogen bonded plane) to form conceptually infinite columns. In the Cambridge Structural Database (CSD, version 5.29, November 2007) there are over 40 structures of **1** that include several common organic solvents. These structures all possess the familiar host architecture, but owing to the presence of a site of $\bar{3}$ symmetry in the centre of the cavity, it is generally not possible to model the guest molecules satisfactorily.

As with other established host systems, several synthetic modifications have been made to **1**. Such alterations include changing the hydrogen bonding functionality (Figure 3.3a) to other groups capable of hydrogen bonding.[7-9] Although the *p*-hydroxyphenyl moiety is regarded as crucial to the formation of the familiar DC architecture, it has been shown that when the hydroxyl group is replaced with a thiol group (compound **2**), an ···S–H···S··· bonded analogue (Figure 3.3b) results and clathrate formation still occurs in the presence of a suitable guest.[9] It is important to note here that, if the guest is not carefully selected, racemic **2** will resolve

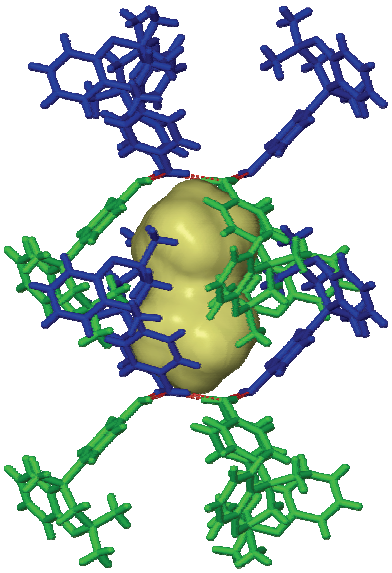

Figure 3.2 The clathrate of DC – enantiomers interdigitate to form an hourglass-shaped cavity (yellow surface). Molecules are shown in capped-stick representation and molecules of opposite chirality have been coloured differently for clarity. Hydrogen bonds are shown as fragmented red cylinders.

spontaneously and crystallise in the chiral space group $P2_12_12_1$.[9,10] Racemic **1** has been resolved synthetically[11,12] and it was revealed that the enantiomerically pure **1** has a similar crystal structure to that of resolved **2**.[13]

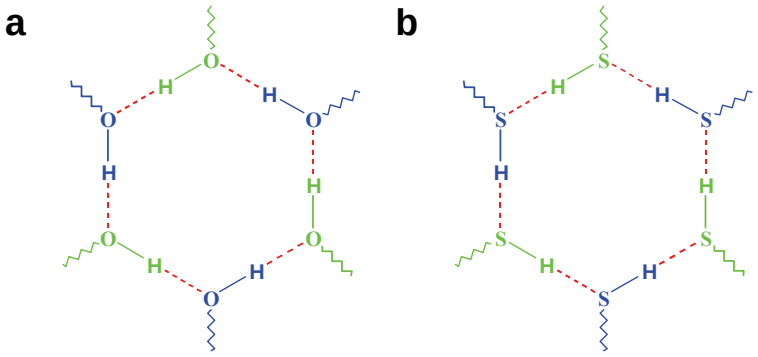

Figure 3.3 **(a)** The well-known hexameric hydrogen bonded ring of DC. **(b)** By changing the hydroxy moiety to a thiol group, it has been shown that the familiar hexagonal ring can also be formed using an ···SH···S··· bonded motif.

In the structure of resolved **2** and the analogous structure of resolved **1**, the familiar ···S–H···S··· and ···O–H···O··· hexameric hydrogen bonded rings are no longer present. Indeed, the enantiomerically pure phase does not appear to form clathrates and crystallises in a close-packed structure with no inclusion of guest or solvent

molecules. Further discussion of the structure will only refer to resolved **2** as the structure of resolved **1** is identical. Molecules of resolved **2** are connected by weak S–H···O hydrogen bonds (S···O distance of 3.489(3) Å) between the chroman and the thiophenol moieties and two adjacent chains are held together by edge-to-face π-π interactions forming double strands (C–H to centroid distance of 3.897 Å) (Figure 3.4). The overall packing can be described as infinitely hydrogen bonded double strands (shown in blue and green in Figure 3.5) organised parallel to the *b*-axis to form a sheet that stacks along [100].

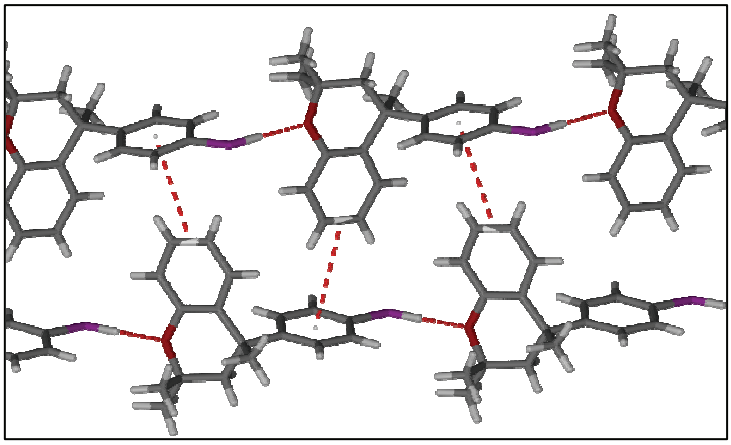

Figure 3.4 Crystal packing of resolved **2** in capped-stick representation showing the intermolecular hydrogen bonding and the π- π interactions as red dashed lines.

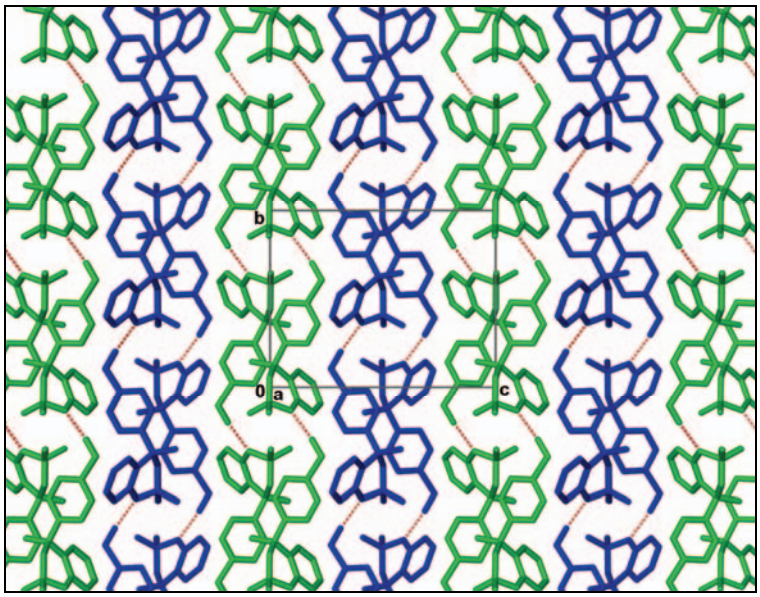

Figure 3.5 Infinite chains of hydrogen bonded molecules extend along [010], with two neighbouring chains forming edge-to-face π-π interactions to assemble a double strand. Each colour here represents one of these double strands.

The study of the gas sorption properties of porous materials is a focus of the Barbour group. It is known that **1** forms the guest-free 'clathrate' structure when the material is sublimed under vacuum at *ca* 110 ºC.[4] Under these conditions, large stable voids of approximately 220 Å^3 are formed in the crystal. These voids are interconnected along the crystallographic *c*-axis by circular apertures of van der Waals diameter 2.50 Å (Figure 3.6a). Only two studies on the gas and vapour sorption abilities of **1** have been reported,[14,15] but we were hesitant to accept these results at face value. In the first study, Barrer and Shanson examined the uptake by **1** of Ar, Kr, Xe, CO_2, CH_4, C_2H_6, C_3H_8, n-C_4H_{10}, iso-C_4H_{10} and neo-C_5H_{12} using volumetric gas sorption techniques. Interestingly, they also reported on the effects of agitating the sample during sorption measurements – *i.e.* that mild crushing of the material improved its ability to sorb more guest molecules. Although the 'pores' between successive voids of **1** are smaller than the adsorbate species in each case, the authors found that guest uptake proceeded nonetheless. Consequently, they suggested that the host framework could not be very rigid in order for guest transport to occur between neighbouring voids. Figure 3.6a shows the hydrogen bonded ring formed by **1** – according to measurements using MSROLL, a sphere of radius greater than 1.249 Å should not pass through the opening. The results reported by Barrer seem peculiar since the authors claimed that molecules as large as n-butane, isobutane and neopentane could

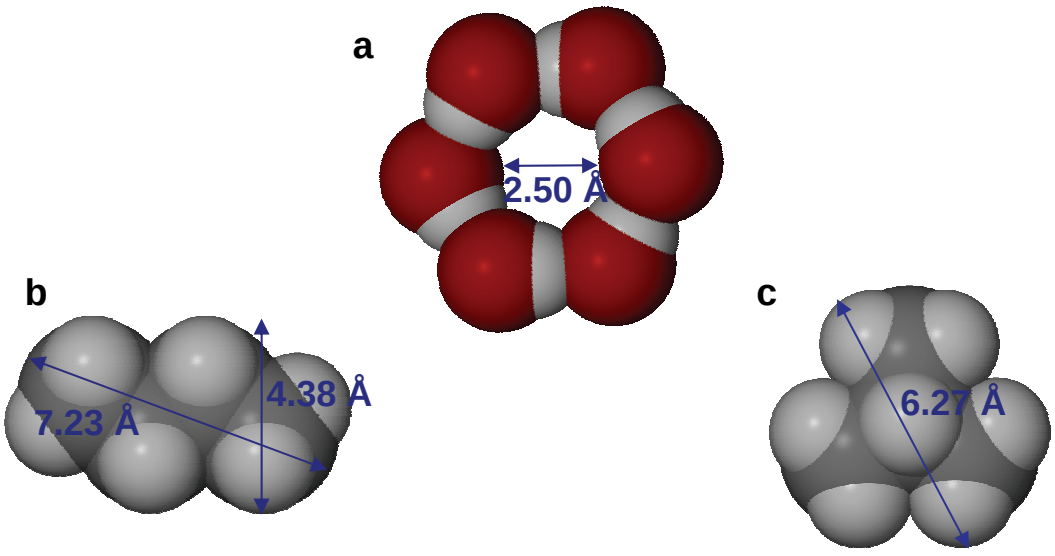

Figure 3.6 Van der Waals representations of **(a)** the hydrogen bonded pore between cavities of **1** **(b)** n-butane and **(c)** isobutane.

be sorbed (Figure 3.6b and c).

In a second account of the sorption ability of **1**, Harrington and Garland[15] reported the uptake of several vapours including methanol, ethanol and acetic acid, even with other guests already present in the cavities. They therefore concluded that sorption by **1** need not only involve uptake of guests into the cavities, but that surface adsorption might also occur. In view of these inconclusive results, we decided to investigate the mechanisms by which sorption (be it surface adsorption or in-cavity absorption) occurs in **1**. In considering the sorption ability of **1** and its analogues, the role of the hydrogen bonded ring guarding the inter-cavity aperture was identified as worthy of investigation. As mentioned above, modification of the hydroxy-group of **1** provides a potential means of controlling the size of the hexameric hydrogen bonded ring. Consequently, it was decided to study the gas sorption ability of the thiol-derivative **2**, as well as a third potential clathrate that will be described in the next paragraph.

We postulated that, by converting the hydrogen bonding functionality of one of the enantiomers of **1** to a thiol moiety, the hexameric hydrogen bonded ring architecture would be maintained (Figure 3.7). In other words, would it be possible to form a quasi-racemic clathrate[16] by co-crystallising one equivalent of one enantiomer of **1** with one equivalent of the opposite enantiomer of **2**? It was believed that, if successful, this would yield an intermediate sized pore for comparison with gas sorption abilities of racemic **1** and racemic **2**. The challenge was thus to crystallise each clathrate in its guest-free form.

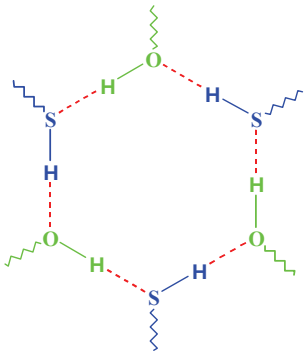

Figure 3.7 A schematic of the proposed ···S–H···O–H··· hydrogen bonded ring as structure-directing feature for forming the desired quasi-racemic clathrate.

The results and discussion of the above-mentioned undertakings follow. The synthetic routes involved in obtaining the components required to test the concept of a quasi-racemic clathrate will be described first, followed by a discussion of the single-crystal structures obtained. Finally, guest desorption experiments and other physical properties will be outlined, including thermal analyses and gas sorption.

3.2 RESULTS AND DISCUSSION

3.2.1 Synthesis and resolution of Dianin's compound and derivatives

In order to investigate the feasibility of preparing the mixed hydroxy-thiol (*i.e.* quasi-racemic) clathrate of DC, the first step was to resolve the (*R*)- and (*S*)-enantiomers of **1**, followed by conversion of one of the enantiomers to the thiol derivative (**2**). The resolution of **1** was achieved by esterification with (1*S*)-(-)-camphanic chloride, after which the resulting diastereomeric mixture was purified by fractional crystallisation from methoxy-ethanol.[11] Hydrolysis of this enantiomerically pure (*S*,*S*)-camphanic ester resulted in chirally pure DC. The other enantiomer of DC was obtained in an analogous manner using (1*R*)-(+)-camphanic chloride as the resolving agent. One of the enantiomers could then be converted to its thiol-derivative *via* the synthesis of a thiocarbamate in a condensation reaction of the hydroxyl moiety of DC and dimethylthionocarbamoyl chloride. This was subsequently converted to the thiocarbamate-derivative and hydrolysed to obtain enantiomerically pure **2**. Detailed synthetic procedures and characterisation follow at the end of this chapter.

3.2.2 Structure determinations by single-crystal X-ray diffraction

In order to test our original hypotheses, *i.e.* whether it is possible to combine one enantiomer of **1** with the opposite enantiomer of **2** and still form a clathrate (which will be referred to as **3**), equimolar amounts of (*R*)-**1** and (*S*)-**2** were dissolved in carbon tetrachloride. Crystals suitable for single-crystal diffraction studies were obtained by slow evaporation of the solvent. The corresponding clathrates of

compounds **1** and **2** were also grown from carbon tetrachloride* and the three different inclusion compounds will be referred to as $\mathbf{1}_{CCl4}$, $\mathbf{2}_{CCl4}$ and $\mathbf{3}_{CCl4}$.

Structure $\mathbf{1}_{CCl4}$ crystallises in the centrosymmetric trigonal space group $R\bar{3}$ with lattice parameters $a = b = 26.8078(12)$ and $c = 10.8706(10)$ Å. Each molecule of carbon tetrachloride is enclathrated by 6 molecules of **1** and is situated within the cavity, but disordered over two crystallographically equivalent positions (Figure 3.8) that are related to one another by $\bar{3}$ site-symmetry. The host molecules are shown in red and the two symmetry-equivalent guest molecules are shown in yellow and green. By considering the space-filling model, it is presumed that the orientation of a guest

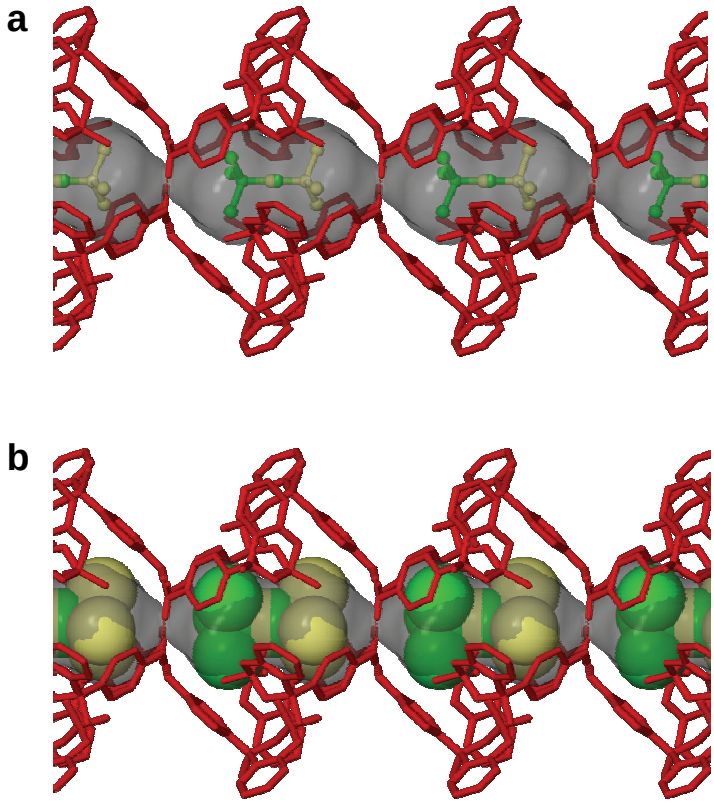

Figure 3.8 Supramolecular assembly of $\mathbf{1}_{CCl4}$ viewed perpendicular to [001]. The racemic host molecules are shown in red and the 50% disordered guest carbon tetrachloride molecules are shown in green and yellow. **(a)** Ball-and-stick and **(b)** van der Waals space-filling models. Six molecules of **1** are joined together by hydrogen bonding (shown as dashed red lines), and stacking of these hexameric units along [001] produces guest-accessible voids (semi-transparent grey surface). All hydrogen atoms, except those of the hydroxy-moieties, have been omitted for clarity.

* These structures had previously been determined, but not at 100 K and the guests had also not been sufficiently well modelled. It was therefore decided to re-determine these structures for comparison to other structures for which we collected intensity data at 100 K.